

Selection of a high affinity peptide ligand binding to a novel functional site of β 2 Integrin p150

Inauguraldissertation
der Philosophisch-naturwissenschaftlichen Fakultät
der Universität Bern

vorgelegt von

Christoph Frick

von Schaan, Fürstentum Liechtenstein

Leiter der Arbeit
PD Dr. Alex Odermatt

Insspital Bern
Abteilung Nephrologie und Hypertonie

Selection of a high affinity peptide ligand binding to a novel functional site of β 2 Integrin p150

Inauguraldissertation
der Philosophisch-naturwissenschaftlichen Fakultät
der Universität Bern

vorgelegt von

Christoph Frick

von Schaan, Fürstentum Liechtenstein

Leiter der Arbeit
PD Dr. Alex Odermatt

Inselspital Bern
Abteilung Nephrologie und Hypertonie

Von der Philosophisch-naturwissenschaftlichen Fakultät angenommen.

Bern, 24. März 2004

Der Dekan:

Prof. Dr. G. Jäger

Part I

1.	Summary	1
2.	Introduction	3
2.1.	β 2 integrins	3
2.2.	β 2 integrin p150 (CD11c/CD18)	5
2.3.	Leukocyte transmigration	6
2.4.	Intercellular adhesion molecules	8
2.5.	Fibrinogen	9
2.6.	Hairy cell leukemia	10
2.7.	Phage-display	11
2.8.	M13 phage	12
3.	Manuscripts and publications	
3.1.	Selection of a high affinity peptide ligand binding to a novel functional site of β 2 Integrin p150	13
3.2.	Selection of peptide ligands binding to the basolateral cell surface of proximal convoluted tubules	
4.	References	36

1. Summary

β 2 integrins are adhesion plasma membrane proteins involved in endothelial and epithelial migration of leukocytes and are therefore potential target molecules to prevent inflammation. Peptide ligands binding specifically to integrins may operate as functional blockers of leukocyte transmigration. Such ligands may also be used for the development of vectors for the targeting of cells expressing specific integrins.

In this work phage-display libraries were screened for peptide ligands binding to purified β 2 integrin p150 (CD11c/CD18), which is so far only poorly characterized. Screening phage-display libraries revealed a phage displaying the circular peptide C-GRWSGWPADL-C. This phage shows several thousand-times higher binding to immobilized p150 than an unspecific control phage. The selected phage failed to bind Mac-1 (CD11b/CD18), a β 2 integrin having 67% homology with p150. Using fluorescence activated cell sorting (FACS) analysis we showed binding of the selected phage to monocytes known to express high levels of p150, in contrast to lymphocytes (negative control) where no specific phage binding was observed. The binding of synthetic peptide C-GRWSGWPADL-C to p150 was examined by Surface Plasmon Resonance (SPR) and a K_D of 20 to 50 μ M was determined.

Intercellular adhesion molecule-1 (ICAM-1) plays an essential role in leukocyte transmigration and is a native ligand of p150. ICAM-1 contains a stretch of amino acid, which is highly homologous with the peptide C-GRWSGWPADL-C. Currently, the epitopes involved in the interaction of both proteins are not known. The phage we selected may help to elucidate the properties of the binding units of p150 and ICAM-1. Moreover, C-GRWSGWPADL-C peptide or variants of it can be tested for prevention of leukocyte transmigration or for targeting p150 positive cells, such as polymorphic mononuclear leukocytes (PMN) or certain blood cancer cells known to express p150.

We also applied the phage-display technique in a project to select peptide ligands binding to the basolateral cell surface of renal proximal convoluted tubules (PCT). Various proteins such as, channels, receptors and transporters, responsible for the absorption of

amino acids, ions, water and glucose from the primary urine are essential in PCT for the proper function of the kidney.

The previous established phage-display method was effectively improved and screenings of phage-display peptide libraries on microdissected intact renal PCT segments resulted in the selection of two phage displaying peptide sequences containing the RDXR motif or the GV(K/R)GX₃(T/S) motif. These phage revealed significant higher binding to microdissected PCT over microdissected cortical collecting duct (CCD), a segment different from PCT and further downstream of the kidney tubular system. Specific phage-binding to PCT was shown by confocal microscopy and by quantitative phage binding assays. The binding of the two phage was abolished by adding the corresponding synthetic peptide in concentrations $\geq 10 \mu\text{mol/L}$. The GV(K/R)GX₃(T/S) motif has homology with the sequence GVKGERGS contained in human collagen- α subunit and was suggested to be its native epitope.

In this biopanning experiment two short peptide motifs were selected and shown to bind specifically to the basolateral side of intact microdissected PCT. Ligands for PCT are relevant for further investigations of cell receptor-ligand interactions. Furthermore, peptide ligands binding to receptors on the cell surface be used for the development of specific viral or non-viral targeting vectors specific for a given tubule segment.

2. Introduction

Integrins are plasma membrane cellular adhesion molecules (CAM) playing an important role in cell-to-cell and cell-to-extracellular matrix (ECM) interactions. Integrins are expressed by all multicellular organisms, but their diversity varies. Humans have 19 α - and 8 β - subunits, whereas *Drosophila* and *Caenorhabditis elegans* expresses only five α and two β subunits [3]. Integrins mediate the attachment of cells to extracellular matrix proteins of the basement membrane or to ligands on other cells. Gene deletion has demonstrated the essential role that integrins play in both the maintenance of tissue integrity and the promotion of cellular migration. Integrin receptors are involved as well in transduction of bi-directional signals between extracellular adhesion molecules and intracellular cytoskeletal and signaling molecules.

Leukocyte extravasation across endothelium, followed by epithelial transmigration is a significant process in inflammatory diseases. Different cellular signalling and adhesion molecules, chemokines and many others are involved in the progression of inflammation. Integrins belong to the key molecules in various adhesion steps during extravasation and transmigration. Many different integrins do exist, whereas $\beta 2$ integrins are of importance in endothelial and epithelial leukocyte transmigration.

2.1. $\beta 2$ integrins

Integrins are transmembrane glycoproteins consisting of two noncovalently linked α - and β -chains, both are type 1 transmembrane proteins (Figure 1). Integrin α -chains consist of a short carboxy-terminal (30-50 amino acids) cytoplasmic domain, a single transmembrane domain and a large globular extracellular domain (700-1000 amino acids) containing a bivalent cation binding site, usually binding calcium or magnesium. The two subunits are held together by non-covalent interactions. In a simplified way the integrin structure can be described as a large head on two legs, with the N-termini of both subunits forming the head responsible for most ligand interactions and the legs formed by the C-termini. Integrins are familiarized determining their β -subunit. 8 different β -subunits and 19 different α -subunits are known. Each sub-family, an individual β -chain, may be associated with several types of α -chains. Not all theoretically possible

combinations occur. Up to now 24 different integrin combinations have been discovered [4].

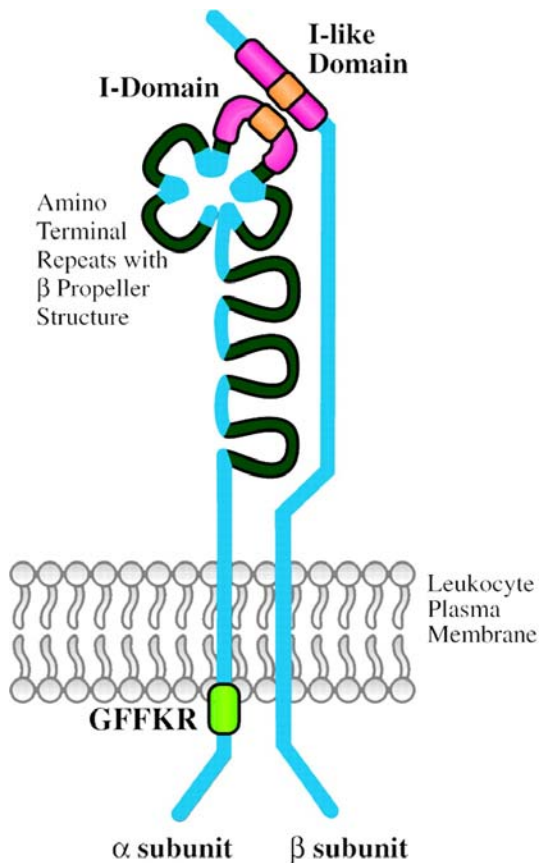


Figure 1

Features of $\beta 2$ integrins. The $\alpha\beta$ heterodimeric structure is common to all integrins. The α chain includes seven extracellular N-terminal homologous repeats organized into a β propeller structure. The α chain I domain is shown in pink with the embedded MIDAS motif in orange, and the β chain I-like domain with MIDAS motif is shown in corresponding fashion. The GFFKR sequence (green) in the cytoplasmic tail of the α subunit is involved in heterodimer assembly and regulation of ligand recognition. The heterodimer is illustrated in the “closed” or inactive state that undergoes tertiary and quaternary changes in response to inside-out signals. (Figure taken from: [1])

$\beta 2$ integrins undergo a conformational change encompassing the phosphorylation of the β -subunit but its contribution to function is not clear. The activation is controlled by the GFFKR site immediately adjacent to the transmembrane domain of the alpha chain. The GFFKR motif serves to lock the heterodimers into a low affinity conformation in the absence of activating signals and is involved in α/β association [5]. Truncations, mutations and deletions of the GFFKR motif in LFA-1 (CD11a/CD18) cause constitutive ICAM-1 recognition. The I domain located in the third β sheet of the α -subunit mediates most ligand binding sites. The N-terminus of the β -subunit possesses an I-like domain. Mutations in this region circumvent ligand binding, indicating its involvement in the binding process. The I domain can adopt two different conformations, an open or “active” and a closed or “inactive” structure [6]. At the top of the α subunit, a Mg^{2+} ion is ligated at a metal-ion-dependent adhesion site (MIDAS). The MIDAS is critical for

switching between the open and closed conformation, which regulate ligand binding. The closed conformation appears in absence of ligand and the open conformation when the I domain is bound to ligand. The MIDAS can alter two of the three loops that undergo a conformational change. The coordination of the metal ion is altered too, which leads then to a more electrophilic environment.

$\beta 2$ integrins are exclusively expressed on leukocytes and are heterodimeric proteins that consist of a distinct α and a common β subunit. The genes of the α subunit of LFA-1 (CD11a/CD18, $\alpha_L\beta_2$), Mac1 (CD11b/CD18, $\alpha_M\beta_2$, complement receptor 3 (CR3)) and p150,95 (CD11c/CD18, $\alpha_X\beta_2$, complement receptor 4 (CR4)) are clustered on chromosome 16p11 (Corbi et al., 1988). The gene for the β subunit which is assessed jointly is located on chromosome 21q22 (Marlin et al., 1986). LFA-1 is expressed on all leukocytes, whereas Mac-1 and p150 are expressed primarily on granulocytes, monocytes and natural killer (NK) cells. The importance of $\beta 2$ integrins in the immune and inflammatory reaction is clearly shown in a disease which is called leukocyte adhesion deficiency (LAD). Patients suffering from this disease lack a correct $\beta 2$ subunit and often have severe bacterial and fungal infections. Neutrophils in this rare inherited disease fail to migrate to inflammatory sites.

2.2. $\beta 2$ integrin p150 (CD11c/CD18)

Functional antibodies raised against CD11c/CD18 effectively block monocyte migration and adherence to endothelial cells [7]. CD11c/CD18 can be induced in promyeloblastic leukemic cell line HL60 incubated with phorbol 12-myristate 13-acetate (PMA) for 48 hours, resulting in markedly increased mRNA levels, showing that its expression is transcriptionally regulated and provoking a differentiation of HL60 cells along the monocytic pathway [8]. P150 binds ligands through the inserted domain (I domain) of the α subunit. Ligands include the complement factor fragment iC3b, fibrinogen and intercellular adhesion molecule 1 (ICAM-1). Site directed mutagenesis of the I domain of the α subunit resulted in an increased affinity up to 200-fold to 2.4 μM compared with wild-type affinity of 400 μM [9]. P150, like other $\beta 2$ integrins, is inactive in resting leukocytes and can be activated after cellular stimulation. Stimulation is not uniform for

all $\beta 2$ integrins, p150 is less sensitive to activation. However, $\beta 2$ integrines are known to be expressed on leukocytes such as granulocytes and monocytes, whereas p150 in particular has an expression distribution among monocytes, macrophages and CD8⁺ subset of dendritic cells [10].

2.3. Leukocyte transmigration

Leukocyte (neutrophils and monocytes) transmigration is an event that must occur at the site of infection as a necessary part of the primary defense mechanism, but excessive accumulation of leukocytes leads to inflammation and tissue damage. Therefore, leukocyte transmigration must be tightly controlled. It is a process that can be subdivided in four steps: 1. leukocyte rolling 2. activation 3. arrest of rolling and adhesion to the endothelial cell layer, and 4. transendothelial migration (Figure 2). Selectins, which belong to a subgroup of CAMs, are responsible for rolling, the initial adhesion and interaction between PMN and endothelium [11]. Antibodies raised against selectins are not able to prevent transepithelial migration of PMN.

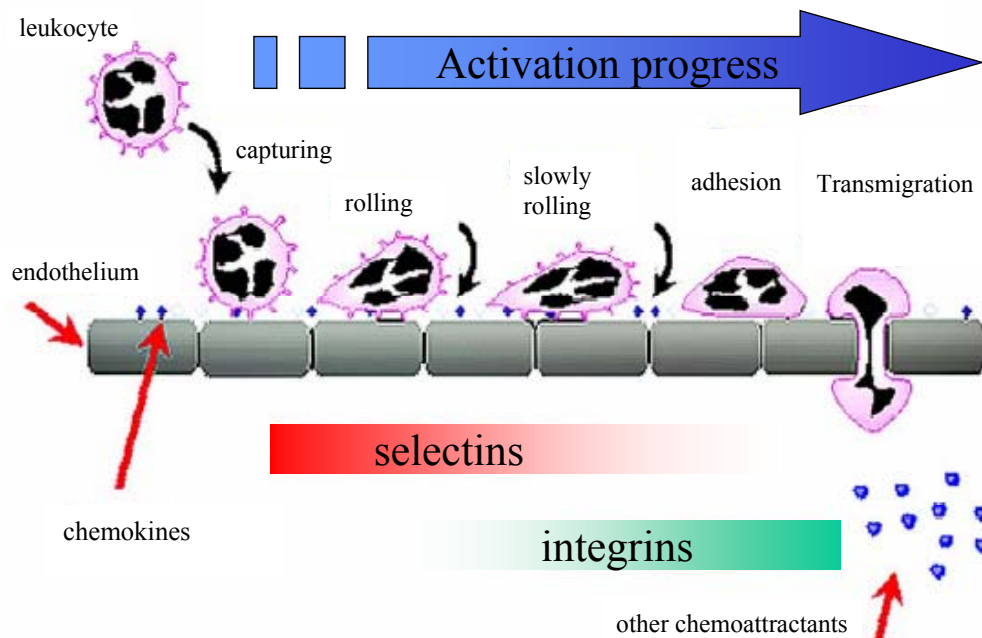


Figure 2 Cell adhesion cascade (Modified from: http://edoc.ub.unimuenchen.de/archive/00001037/01/Hundelshausen_Philipp_von.pdf)

Activation is mediated by chemoattractants, including chemokines and other molecules. Binding of these chemoattractants results in a G-protein-mediated activation signal, which causes a large increase in the affinity of the integrin molecules on the leukocyte membrane. Intercellular adhesion molecule-1 (ICAM-1) is a binding partner located on the apical side of the endothelium of PMA expressing LFA-1 and Mac-1. The increased affinity of the integrin molecules causes the leukocyte to bind tightly to the ICAM-1 molecules on the surface of the endothelial cells (step 3 of leukocyte transmigration).

Adhesion Molecule	PMN-Epithelium	PMN-Endothelium
CD11a/CD18 (LFA-1)	-	+
CD11b/CD18 (Mac-1)	+	+
CD11c/CD18 (p150)	+/- ?	+/- ?
CD11d/CD18	?	?
CD47	+	+
CD31(PECAM)	+	+
CD54 (ICAM-1)	- ^a	+
CD62L (L-selectin)	-	+
CD62E (E-selectin)	-	+
CD62P (P-selectin)	-	+
Other (carbohydrate-mediated)	+	+

Table 1. Contrasting adhesive interactions during neutrophil (PMN) transepithelial and transendothelial migration

^aFollowing cytokine stimulation or bacterial exposure, epithelia express CD54 (ICAM-1) on the apical epithelial surface, where it may serve as a PMN adhesive receptor. Apical compartmentalization of this receptor, however, precludes it from being used as a PMN receptor during the process of transepithelial migration.

Table taken from Jaye & Parkos, 2000

Extravasation is the last step in the process of leukocyte endothelial transmigration.

As table 1 shows $\beta 2$ integrins are of relevance for PMN migration across endothelia and epithelia. PMN from leukocyte adhesion deficiency (LAD) patients, who lack $\beta 2$ integrins, fail to migrate through endothelia [12]. Ex vivo molecules, antibodies and chemoattractants can be tested to block epithelial and endothelial PMN transmigration in a migration assay chamber system as described by Parkos and Jaye [13]. PMN move across the epithelial cell layer from the basolateral epithelial membrane, through the paracellular space, and finally they pass the tight junctions. Epithelial cell lines such as T84 are grown to confluence on permeable filters with pores which allow PMN to transmigrate to the other chamber. The system may be set up in an apical-to-basolateral direction adding PMN to the upper chamber and chemoattractants to the lower chamber. To study the physiological relevant migration, which is from the basolateral-to-apical side, PMN have to be added into the lower chamber and chemoattractants into the upper chamber.

Using such an approach as a model system, peptide-ligand binding receptors, which are involved in endothelial and epithelial PMN transmigration, can be tested for functionality, helps to elucidate the features of molecules contributing to PMN migration.

2.4. Intercellular adhesion molecules (ICAM)

ICAM's normally function to promote intercellular adhesion and signalling. The N-terminal domain of the receptor binds to the rhinovirus "canyon" surrounding the icosahedral 5-fold axes, during the viral attachment process. ICAM family belongs to the Ig superfamily and is therefore related to the family ig. Five different ICAMs are known, designated as ICAM-1 to ICAM-5 and are known to bind leukocyte $\beta 2$ integrins (CD11/CD18) during inflammation and in immune responses. ICAMs are highly glycosylated type 1 transmembrane proteins. In addition, ICAMs may exist in soluble forms in human plasma, due to activation and proteolysis mechanisms at cell surfaces.

ICAM-1 (CD54) has a molecular weight of 57826 Daltons and contains five Ig-like domains. It is expressed on leukocytes, endothelial and epithelial cells and is upregulated in response to bacterial invasion. ICAM-1 is a ligand for lymphocyte-function associated 1 (LFA-1) antigens, fibrinogen [14], the major group of human rhinoviruses [15], *Plasmodium falciparum* [16], and also a receptor for $\beta 2$ (CD11a/CD18 and

CD11b/CD18). ICAM-1 has been suggested to be a counterreceptor for p150 (CD11c/CD18) [17].

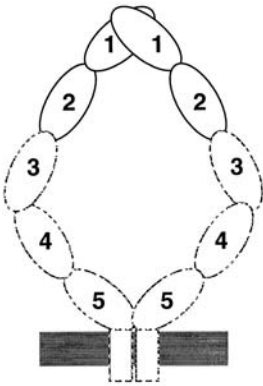


Figure 3
A model for the ICAM-1 dimer on the cell surface. Domains 1 and 2 and their orientation in the dimer are derived from the crystal structure.
(Figure taken from Casanovas et al., 1998[2])

The first domain of ICAM-1 binds to LFA-1 and the second domain of ICAM-1 has a role in maintaining the structure of the LFA-1 ligand-binding site in the first domain [18]. The binding sites of all of its other binding partners has been located in the first domain and the binding sites were different or overlapping [18]. Domain 1 and 2 of ICAM-1 were crystallized and a model for an ICAM-1 dimer was suggested as shown in Figure 3 [2].

2.5. Fibrinogen

Fibrinogen is a major blood plasma protein which is converted into fibrin to prevent blood leaks from blood vessels [19]. Besides blood clotting, fibrinogen is involved in additional functions such as platelet aggregation, leukocytes adhesion, and stimulation of cytokine release in macrophages [20]. Fibrinogen can be cleaved into two types of fragments by plasmin, which are called, fragment E and fragment D. Mac-1 and p150 bind to fragment D and fragment E, respectively. Fibrinogen is a ligand for both Mac-1 (CD11b/CD18) and p150 (CD11c/CD18). The two β 2 integrins recognize different sites of the fibrinogen molecule even though they have quite similar molecular structure. The I-domain of p150 is the binding partner for fibrinogen.

2.6. Hairy cell leukemia

Hairy cell leukemia (HCL) is a malignant cancer disease in which tumor cells are found in the blood and bone marrow. The disease is called hairy cell leukaemia because these cancer cells look “hairy” when viewed under the microscope. HCL is a rather rare cancer and was first described in 1958 as leukemic reticuloendotheliosis. About 600 new cases are diagnosed every year in the United States that is about 2 % of the adult cases of leukaemia each year. HCL specifically affects B-lymphocytes, which mature in the bone marrow. When HCL develops, the B-lymphocytes become abnormal in the way they appear (hairy) and in the way they act (proliferating without the normal control mechanisms). HCL cells tend to accumulate in the spleen and express high levels of p150 (CD11c/CD18). Therefore spleens from HCL patients are taken as source for the purification of p150 [21].

Patients suffering from HCL have limited production of normal white blood cells and may have frequent infections. Infections of any kind are the major cause of death of HCL patients. Some individuals with HCL have very few or no symptoms at all. There are three possible treatments: splenectomy (removal of spleen), immunotherapy (interferon) and chemotherapy. Most commonly used chemotherapeutic substances are purine analogues, particularly pentostatin and cladribine. Most patients have relatively good prognosis and life expectancy is 10 years or longer. The disease may remain silent for years with treatment.

Source: http://www.healthatoz.com/healthatoz/Atoz/ency/hairy_cell_leukemia.html
<http://www.nlm.nih.gov/medlineplus/print/druginfo/medmaster/a692004.html>

2.7. Phage-display

Phage display technology was first applied to display (name) proteins or peptides from monoclonal antibodies on the surface of bacteriophage particles. The phage display method was then improved and used as a tool for screening proteins or peptides displayed on phage, a process called biopanning (Figure 4). Such peptide display libraries can be screened for various properties of interest, including the ability to bind to purified target molecules or specific target cells.

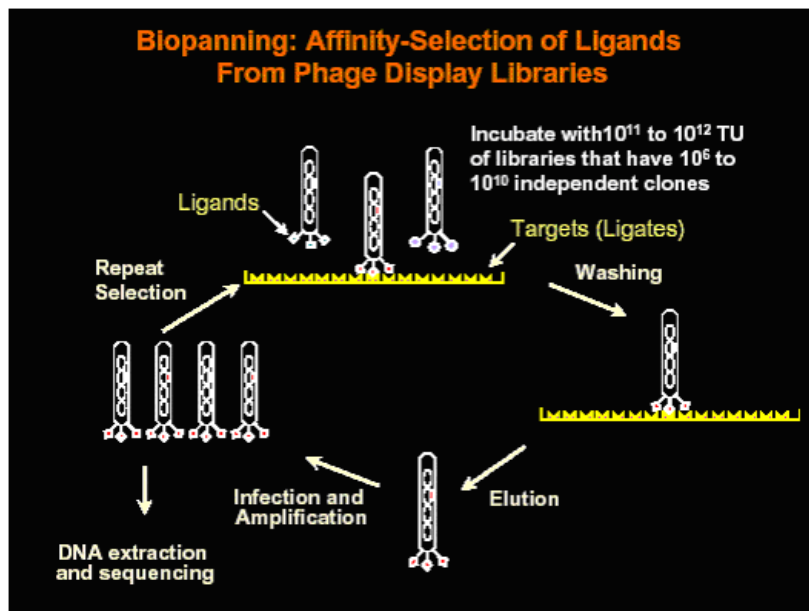


Figure 4
Schematic
representation of the
phage-display
method

Source:
<http://www.niddk.nih.gov/fund/other/genoproto/wang.pdf>

Phage display describes an *in vitro* selection technique in which a peptide or protein is genetically fused to a coat protein of a bacteriophage. This physical linkage between the displayed protein and the DNA encoding it allows screening of a huge number of different protein, which are linked to its corresponding DNA. The first step of a biopanning procedure is incubating the library (a pool of various phage) with the target molecule immobilized on a surface. The unbound phage are then washed away. Afterwards the bound phage can be eluted by low pH or specifically by ligands toward the immobilized target or antibodies. The eluted phage are then amplified in *E. coli* and reapplied to immobilized target molecule for a further round of selection. This procedure results in an enrichment of specific phage binding the target molecules. After several rounds of panning (usually 3-5) phage DNA is isolated, sequenced and individual clones are analyzed.

2.8. M13 phage

Several phage have been used for phage display expression, including the filamentous phage M13, T7 and T4. M13 is probably the most widely-used system. These phage are about 900 nm long and 9 nm wide and consist of only 5 different proteins (Figure 5).

The major coat protein is expressed by gene 8 (g8p) and there are approximately 3000 copies of this protein per phage, together with minor capsid proteins g3p, g6p, g7p and g9p approximately 5 copies of each, which are located at the very end of the filamentous particle. The genome of M13 is 6.4 kbp long. To create M13 phage display libraries mainly the gene coding for g3p and g8p are modified.

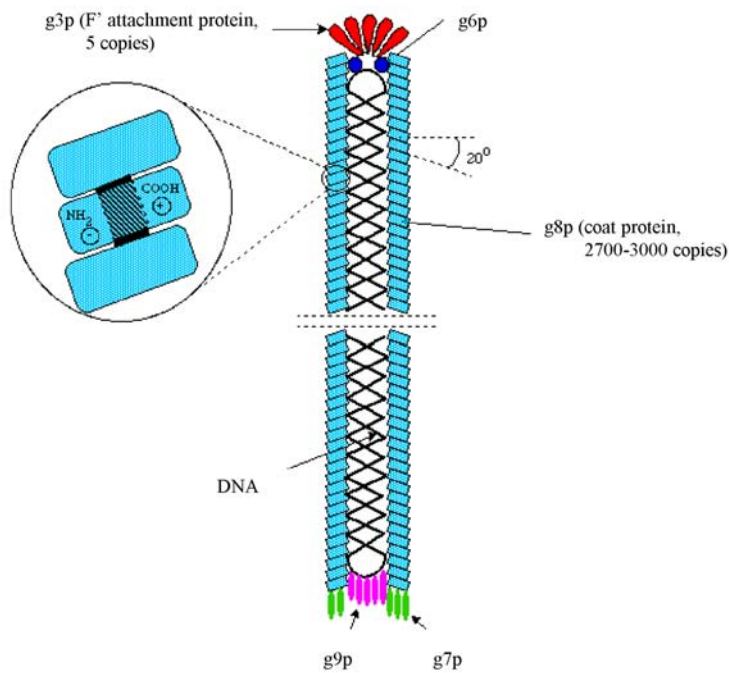


Figure 5

M13 bacteriophage
used for phage-display
screening

Source: <http://www-micro.msb.le.ac.uk/224/Phages.html>

In the present project, two different libraries were used. In library LL9 linear random nonapeptides were fused to the N-terminal end of the g3p protein, whereas in library CL10 two cysteins residues flanking the random decapeptides allowed circular display of the peptides at the tip of the M13 phage [22]. The use of linear and circular libraries in the screening for high affinity binding motifs has proven to be useful since the distinct conformation of the peptide motif often is critical for binding specificity.

Selection of a high affinity peptide ligand binding to a novel functional site of β 2 Integrin p150

Christoph Frick¹, Alex Odermatt¹, Heather Edens³, Ke Zen³, Cissy Geigerman³, Reto Portmann⁴, Ross E. Fuller³, Luca Mazzucchelli², David L. Jaye³, and Charles A. Parkos³

¹Division of Nephrology and Hypertension, Department of Clinical Research, University of Berne, Switzerland

²Institute of Pathology, University of Berne, Switzerland

³Department of Pathology and Laboratory Medicine, Emory University School of Medicine, Atlanta, Georgia

⁴Department of Clinical Pharmacology, University of Berne, Switzerland

Correspondence to: Charles A. Parkos, Department of Pathology and Laboratory Medicine, Emory University School of Medicine, Atlanta, Georgia
E-mail: cparkos@emory.edu

Summary

Integrin p150 (CD11c/CD18) is expressed at high levels in certain hematopoietic malignancies and plays a role in leukocyte and cell matrix adhesion. However, its physiological function is poorly characterized. Here we describe the identification of a phage expressing a circular peptide with the sequence C-GRWSGWPADL-C that was selected screening a phage display peptide library using purified p150. Phage bearing this peptide showed 10^3 -fold higher binding to p150 than control phage.

The selected C-GRWSGWPADL-C phage failed to bind to purified Mac-1 (CD11b/CD18). It bound specifically to monocytes expressing p150 but not to p150 negative lymphocytes. The synthetic circular peptide C-GRWSGWPADL-C bound to purified p150 with a K_D of 20-50 μ M but did not bind to Mac-1. The synthetic peptide was unable to displace the phage from p150, suggesting that multimeric display is essential for high affinity binding of the phage. Neither Fibrinogen nor anti-p150 antibody 4G1 significantly reduced binding of C-GRWSGWPADL-C phage to p150, indicating that this motif mediates binding to a novel and potentially functional site on p150. This motif may be used as a marker, or for the development of delivery vectors targeting p150 positive cells.

Introduction

Leukocyte extravasation across the endothelium, followed by epithelial transmigration is an essential process in inflammatory diseases. Various cellular signaling and adhesion molecules, chemokines and other regulatory factors are involved in the progression of inflammation. Integrins belong to the molecules playing a key role in various steps during extravasation and transmigration. While circulating in blood or lymphatic vessels, leukocytes are in a resting or low adhesive state. However, when stimulated by signals from the immune system, integrins on the surface of leukocytes are activated. During activation, integrins undergo a conformational change involving the I-domain, which is part of the α -subunit [9]. In resting leukocytes, low affinity integrins are equally distributed over the plasma membrane. Upon activation, integrins can bundle within seconds and act locally as high affinity spots. Integrins consist of an α -subunit and a β -subunit, whereby many different combinations are known. $\beta 2$ integrins are of relevance for neutrophil migration across endothelia and epithelia. They have a common β -subunit, CD18, but vary in their α -subunit [23]. LFA-1 (CD11a/CD18) is known to be involved exclusively in neutrophil endothelial transmigration, whereas Mac-1 is of importance for neutrophil and endothelial and epithelial transmigration [13].

To identify specific peptide ligands binding to various integrins, Ruoslahti and coworkers applied phage-display to screen peptide libraries for ligands binding to purified integrins as well as to intact cells expressing integrins [24]. These screenings often resulted in the selection of peptide ligands containing the conserved RGD motif. The RGD motif mediates binding to $\alpha_5\beta_1$, $\alpha_v\beta_3$, $\alpha_v\beta_5$, and $\alpha_{11b}\beta_3$ integrins. Koivunen et al. [25] identified a peptide LLG-C4 that mediated binding to $\beta 2$ integrins. They showed inhibition of leukocyte cell adhesion by adding the synthetic peptide LLG at a concentration of 1 mM. In contrast to the well characterized Mac-1, little is known on the role of p150 in leukocyte adhesion and in transmigration. p150 is expressed at high levels in certain hematopoietic malignancies and plays a role in leukocyte and cell matrix adhesion. Here, we describe a peptide ligand binding specifically to p150 but not Mac-1. This novel ligand should be useful for the elucidation of the function of p150 in future experiments.

Methods

Screening of phage display peptide libraries

In experiments 1, 2, 4 and 5, purified p150 was diluted in HANKS buffered salt solution, pH 7.4, coated onto wells at 0.5 µg/well (polysorb 96-well microtiter plate, NUNC-IMMUNO PLATE, Life Technologies, Merelbeke, Belgium) for 2 h at 37°C. Experiment 3 was conducted with purified Mac-1 bound to sepharose beads. Incubation was for 4 h at 4°C, followed by washing twice with incubation buffer and six times with HANKS buffer containing 0.2% octylglucoside. Microtiter wells were washed with incubation buffer (HANKS, pH 7.4, containing 0.1% heat inactivated BSA and 0.05% octylglucoside) to remove unbound protein. Biopanning in microtiter wells was performed in a total volume of 100 µl and panning on beads in 1 ml, containing 10¹⁰ transducing units (TU) of library CL10 displaying random decapeptides with a structural constraint imposed by a disulfide bond between two cysteins residues flanking the variable region, or library LL9, displaying linear random nonapeptides [22]. In experiment 1 and 3 bound phage were eluted with 100 µl of 20 mM sodium EDTA, pH 7.4; in experiment 2 elution was by adding 0.2 µg of anti Mac-1 antibody CBRM1/29; and in biopanning 4 and 5 bound phage were eluted with 0.9% NaCl, 100 mM glycine, pH 2.2, followed by neutralization of the pH by adding 100 µl of 200 mM sodium bicarbonate, pH 7.4. Eluted phage were amplified in K91 *Escherichia coli* as described [26] An aliquot of 10¹⁰ TU was reapplied in a subsequent round of panning. After the fourth or fifth round of panning, single-strand DNA was prepared from individual phage clones and the unique nucleotide region of the pIII protein encoding the random peptide was sequenced using the oligonucleotide primer 5' GTTTTGTCGTCCTTCCAGACG 3'.

Phage binding assay

Purified p150 (0.5 µg/well) or Mac1 (5 µg/well) were coated onto microtiter wells as described above. Integrins were incubated with 10⁸ TU of the corresponding phage for 4 h at 4°C. After extensive washing with HANKS buffer, pH 7.4, containing 0.05% octylglucoside, bound phage were eluted with 100 µl of 0.9% NaCl, 100 mM glycine, pH 2.2, followed by neutralization of pH as described above. Phage titer was determined by

plaque assay as described earlier [27]. Data are presented as mean \pm SD and were obtained from four independent experiments.

Competition assay

Purified p150 (0.5 μ g/well) was coated as described above and pre-incubated for 10 min at 25°C with various concentrations of fibrinogen, ranging from 100 pM to 1 mM, or with various concentrations of synthetic C-GRWSGWPADL-C, ranging from 100 pM to 100 μ M. Phage (10^8 TU) were then added, followed by incubation for 2 h at 4°C. After extensive washing with HANKS, pH 7.4, containing 0.05% octylglucoside, bound phage were eluted as described above and phage titer was determined by plaque assay. Data were obtained from three independent experiments. Data are given as mean \pm SD.

Surface Plasmon Resonance

All BIAcore experiments were performed on CM5 chips with continuous flow of HANKS, pH 7.4, containing 1% octylglucoside. The surface of a CM5 chip was activated by injecting 50 μ l of *N*-hydroxylsuccinimide/*N*-hydroxylsuccinimide (NHS) and 1-ethyl-3-(3-dimethylaminopropyl) carbodiimide (EDC) with a flow of 5 μ l/min, resulting in a baseline of approximately 13000 RU. The activated chip was then coated with 80 μ l of a solution containing 500 ng of purified p150 in 50 mM potassium acetate, pH 5.0, 2 mM MgCl₂, 2 mM CaCl₂, and 1% octylglucoside, by injection with a flow of 5 μ l/min, giving a typical signal increase of about 5000 RU. Excess reactive groups were deactivated by injecting 30 μ l of 1 M ethanolamine, pH 9.0, within 6 min. In a typical BIAcore experiment, various concentrations of ligands were analyzed with a flow of 5 μ l/min, giving an association and dissociation time of 2 min each, followed by injection of TAE wash buffer (Tris 50 mM, EDTA 0.1 M, pH 11.5). Analyzed ligands were diluted in HANKS buffer, pH 7.4, containing 1% octylglucoside. The interacting proteins were released from p150 on the CM5 chip by washing with buffer TAE, containing 1% octylglucoside.

The data analysis was performed by using the BIAevaluation version 3.1 software (BIAcore). All analyzed interactions were assumed to follow pseudo-first order kinetics.

The calculated association (k_a) and dissociation (k_d) rates were derived by fitting the biosensor curves. K_D was calculated from the relation $K_D = k_d/k_a$.

Fluorescence-activated cell sorting (FACS)

Human mononuclear blood cells were isolated from healthy volunteers and flow cytometric immunophenotyping was performed essentially as described [28], [29]. Cells were analyzed on a FACSort cytometer (Beckton Dickinson, San Jose, CA). At least 10,000 events were measured. Data acquisition and analysis were accomplished using Cellquest software, version 3.1 (Beckton Dickinson, San Jose, CA). Standard criteria were used for placing gates on different hematopoietic cell populations.

M13 phage was detected using anti-M13-biotin antibody (Serotec Inc, Raleigh, North Carolina) and streptavidin- PE antibody (Jackson Laboratories, Bar Harbor, Maine). P150 was detected with mouse monoclonal anti-p150 antibody 4G1 [21] and Alexa-488 anti-mouse IgG antibody.

Results

Selection of phage binding to Mac-1 and p150

In a search for peptide ligands binding specifically to β 2 integrin p150 (CD11c/CD18) or Mac-1 (CD11b/CD18), the circular decapeptide library CL10 and the linear nonapeptide library LL9 were screened using purified integrins. Biopannings were performed using either purified integrins coated onto polysorb microtiter wells or, alternatiely, on sepharose beads. After the fourth or fifth round of panning several phage were sequenced (Table I). Panning on Mac-1, performed on polysorb strips screening library LL9, yielded phage expressing peptides with the consensus sequence MDKXH. Phage MDNGTKRRL and RIFSDKHPP have an incomplete motif. The sequence of the peptide displayed by eight individual phage was determined. Elution was with 20 mM EDTA. In similar pannings using circular library CL10, phage bearing peptides with the MDKXH motif were absent (not shown). From a panning performed on Mac-1 using the circular library CL10, phage with a consensus motif WRS were selected. Surprisingly, among the eight phage analyzed from this panning, one phage with an inverted WRS motif (C-WTAPGSRWEV-C) was selected. In this biopanning experiment phage were eluted with antibody CBRM1/29, a partial blocker of Mac-1. In addition, we performed pannings with Mac-1 coated to beads. Two independent experiments yielded, phage expressing two different sequences, the linear nonapeptide AHKSARKTE or WSYWETVAK. Elution of the phage was with 5 mM EDTA. In the first panning 9 of 10 phage had the same sequence AHKSARKTE, whereby the nucleotide sequence was identical, indicating that they were derived from one original phage clone.

Two independent pannings performed with coated p150 using the circular library CL10 yielded exclusively phage with the sequence C-GRWSGWPADL-C. The phage were eluted with low pH. Sequencing phage after the fourth round of panning did not yield C-GRWSGWPADL-C phage or phage containing a partial motif. A second panning experiment with circular library CL10 and p150 yielded 5 out of 10 sequenced phage displaying the circular peptide C-HKGHDRGKK-C.

Circular phage C-GRWSGWPADL-C binds specifically to p150

To assess the specificity of the selected phage, we incubated Mac 1 (Figure 1A) and p150 (Figure 1B) with purified selected phage. Selection on Mac-1 did not lead to the identification of a high affinity binding phage. None of the phage selected on Mac-1 bound significantly better to Mac1 than control phage F2. Phage C-GRWSGWPADL-C, selected on p150, showed about a ten-fold higher binding to Mac-1 compared with control phage F2, which displays two random amino acids (RV). The same set of phage was tested to bind to p150. None of the selected phage showed significant binding to p150 except phage C-GRWSGWPADL-C, which showed approximately 5000 fold higher binding to p150 than the control phage. Phage C-HKGHDRGKK-C, which is a peptide selected from an independent panning on p150 did not show specific binding to p150. Binding of phage C-GRWSGWPADL-C to uncoated wells (No) was not detectable.

Synthetic peptide C-GRWSGWPADL-C and fibrinogen could not compete for binding of C-GRWSGWPADL-C phage to p150

We further investigated binding of circular phage C-GRWSGWPADL-C to p150. Fibrinogen is a known ligand for p150; thus, in a competition assay binding of C-GRWSGWPADL-C phage was analyzed in the presence of various concentrations of fibrinogen. P150 was preincubated with fibrinogen, ranging from 1 pM to 1 mM. After 10 min, C-GRWSGWPADL-C phage or F2 control phage were added. Fibrinogen did not affect C-GRWSGWPADL-C phage binding at any concentration. The increased binding of C-GRWSGWPADL-C phage and F2 control phage observed at high concentrations of fibrinogen ($\geq 100 \mu\text{M}$) may be due to unspecific binding at high total protein concentrations. Binding of control phage was several orders of magnitude lower at all fibrinogen concentrations than binding of C-GRWSGWPADL-C phage.

Synthetic peptide C-GRWSGWPADL-C binds to p150

Binding of synthetic peptide C-GRWSGWPADL-C to p150 was measured by surface plasmon resonance. The CM5 chip surfaces were coated with purified p150 followed by a constant flow with a solution containing synthetic peptide C-GRWSGWPADL-C (1,332

kDa). Peptide C-GRWSGWPADL-C bound to p150, resulting in an association phase and a dissociation phase (Figure 3 B), whereas the control BSA and the circular control peptide C-ELRGDMAAL-C did not bind to p150 (data not shown). A K_D of 20 to 50 μM was obtained for peptide C-GRWSGWPADL-C. We next analyzed binding of fibrinogen (340 kDa) to immobilized p150. Binding of fibrinogen to p150 resulted in a typical receptor – ligand binding curve, with an association, saturation and dissociation phase. A K_D of 20 nM was determined for fibrinogen. In contrast to the rather weak signal obtained with the small peptide C-GRWSGWPADL-C binding of fibrinogen, which is about 250 times higher, resulted in a more pronounced interaction signal. Binding of peptide C-GRWSGWPADL-C to p150 was specific since no signal was detected when Mac-1 protein was coated onto the surface plasmon resonance chip.

Circular peptide C-GRWSGWPADL-C could not be coated onto the CM5 chip because of lack of an amine group for immobilization. Also C-GRWSGWPADL-C phage did not result in a typical binding phase with association and dissociation, when applied on p150 coated on the CM5 chip.

C-GRWSGWPADL-C phage binds specifically to monocytes

Monocytes and a subset of lymphocytes, NK-like, express high levels of p150. Binding of C-GRWSGWPADL-C phage to these cell types was tested by Fluorescence Associated Cell Sorting (FACS). As shown in Figure 4, monocytes and a small subset of lymphocytes shift with C-GRWSGWPADL-C phage, consistent with the known pattern of p150 expression and indicating that C-GRWSGWPADL-C phage binds to p150 positive cells. In contrast, the main population of lymphocytes, which do not express p150, were not shifted by C-GRWSGWPADL-C phage. We next tested whether synthetic C-GRWSGWPADL-C peptide inhibits C-GRWSGWPADL-C phage binding to monocytes and the NK-like subset of lymphocytes. Neither 1 mM of peptide C-GRWSGWPADL-C nor 1 mM of control peptide inhibited binding of C-GRWSGWPADL-C phage, indicated by the similar pattern obtained for the control in absence of peptide C-GRWSGWPADL-C (not shown). Mean fluorescent intensities were not statistically different. Anti-CD11c antibody 4G1, known as a partial functional blocker of p150, was tested in FACS analysis to inhibit C-GRWSGWPADL-C phage

binding (Figure 5). Antibody 4G1 failed to inhibit C-GRWSGWPADL-C phage binding to both cell types tested in comparison to a control incubation with anti-CD14 antibody (Figure 5A and B). Simultaneous staining of antibody 4G1 and C-GRWSGWPADL-C phage (Figure 5C) or of control anti-CD14 antibody and C-GRWSGWPADL-C phage (Figure 5D) shows that binding of C-GRWSGWPADL-C phage and anti p150 antibody 4G1 is directly proportional. Anti-CD14 antibody binds exclusively to monocytes. Comparison with the binding of C-GRWSGWPADL-C phage indicate that the findings in Figure 5C are not merely due to inadequate compensation. These results suggest that phage C-GRWSGWPADL-C and antibody 4G1 bind to non-overlapping sites on the same cell.

Discussion

Here we describe the selection of a highly specific peptide ligand for the leukocyte $\beta 2$ integrin p150 (CD11c/CD18) using the phage-display screening method. Phage displaying circular peptide C-GRWSGWPADL-C bound with high affinity to purified p150 but failed to bind to purified Mac-1 (CD11b/CD18). We have further shown that this phage specifically mediated binding to monocytes known to express high levels of p150 but not to lymphocytes not expressing p150.

P150 and Mac-1 both possess a common β subunit (CD18) but a different α -subunit, which is about 63% identical in its amino acid sequence [21]. The specific binding of C-GRWSGWPADL-C phage to p150 suggests binding to the CD11c α -subunit of p150. Our results indicate that the multimeric display of the five copies of C-GRWSGWPADL-C peptide attached to the pIII protein at the tip of the phage are critical for high affinity binding to p150 since the synthetic peptide C-GRWSGWPADL-C was unable to displace C-GRWSGWPADL-C phage from purified p150 or from monocytes expressing high levels of p150. The reason for this is not clear, it may be due to differences in the conformation of the peptide ligand when expressed on the phage surface compared to the free peptide in solution or, alternatively, this effect may be explained by the high local concentration of the peptide when five copies are displayed at the tip of the phage. Assuming that the five copies of the peptide are located in a volume of about (10 nm^3), the local concentration of the peptide at the tip of the phage may reach up to 10 mM, exceeding the concentration of the applied monomeric synthetic peptide ($100 \mu\text{M}$) by a factor 100. In surface plasmon resonance experiments the synthetic peptide C-GRWSGWPADL-C bound specifically to purified p150 with a K_D of 20 to $50 \mu\text{M}$. Since the multimeric display of the C-GRWSGWPADL-C peptide seems to be critical for high affinity binding, the C-GRWSGWPADL-C peptide might be displayed on dendrimers or inserted in liposomes in future experiments investigating the physiological effect of this peptide motif. Binding of C-GRWSGWPADL-C phage to p150 could not be assessed by surface plasmon resonance. The size of the phage might be too large (900nm) to fully protrude in to the diffusion area of the chip and allow binding to the coated p150. The surface plasmon resonance RU amplitude obtained with fibrinogen (340 kDa) was much

more intense than that of the, C-GRWSGWPADL-C peptide (1.332 kDa), due to the high size difference. The high affinity synthetic binding of fibrinogen with a K_D of 20 nM demonstrates that the p150 coated on the chip was in a functionally active conformation. Vorup-Jensen et al. [9] reported a K_D of 400 μ M of the p150 ligand iC3b in a surface plasmon resonance protein interaction experiment. A mutation which caused a conformational change in the I-domain C-terminal helix, increased the affinity up to 200-fold.

Biopanning using Mac-1 did not yield any peptide motif that mediated significantly increased binding to Mac-1. Phage bearing the MDKXH or WRS motif had low affinity for Mac-1 and did not distinguish between Mac-1 and p150 did not observe any phage bearing the LLG motif described by Koivunen et al. Whether this is due to the different constraint by the CX₇C and CX₉C library used by the present study remains to be investigated. Mac-1 and p150 are the main receptors for fibrinogen expressed on neutrophils, monocytes, macrophages and several subsets of lymphocytes. Despite of the high similarity between Mac-1 and p150, they recognize different regions of fibrinogen. The CD11c I-domain binds fibrinogen, whereby the binding is dependent on divalent cations (Sang-Uk Nham, 1999). Our experiments indicate that fibrinogen and C-GRWSGWPADL-C phage bind to different epitopes on p150 since fibrinogen was not able to prevent binding of C-GRWSGWPADL-C phage binding to purified p150. Antibody 4G1, a partial blocker of p150 function and recognizing the α -subunit (CD11c) and did not inhibit C-GRWSGWPADL-C phage binding. Binding experiments by Stacker and Springer [21] with chimeric molecules of CD11b and CD11c located the 4G1 binding site on CD11c of p150 between the third divalent cation binding domain and the C-terminus. This experiment suggests that the region downstream from I-domain of CD11c has functional properties as well. The simultaneous detection of the binding of C-GRWSGWPADL-C phage and antibody 4G1 to monocytes expressing p150 suggests that they bind to independent sites on p150. In addition, the FACS experiments demonstrate that C-GRWSGWPADL-C phage recognizes an epitope which is accessible under native conditions.

ICAM-1 is a rather poorly characterized ligand to p150 (Diamond, 1993), and neither the p150 nor the ICAM-1 sites involved in the binding are known. Alignment of the peptide

sequence with that of ICAM-1 reveals a highly homologous motif in ICAM-1 (CD54) upstream of its fifth IG domain, a region for which no binding properties have been described so far (Figure 6). Four of six amino acids are identical. Amino acids that are different have similar side chains, e.g. serine and threonine (OH) or asparagines and arginine (NH₂), respectively. Based on the sequence comparison we hypothesize a disulfide bridge between cysteine 403 and cysteine 419 that would allow a phage-like circular display of the sequence in ICAM-1. Interestingly, the SwissProt database predicts a disulfidebridge between cysteine 419 and cysteine 457 suggested by similarity analysis. Domain one and partially domain two of ICAM-1 are responsible for binding to LFA1 (CD11a/CD18) (Staneley, 2000). Koivunen et al. [25] successfully selected a phage displaying a peptide with the motif LLG from a panning performed on Mac-1. LLG is part of the sequence of the IG domain one of ICAM-1 and of von Willebrand factor. Domain one and two of ICAM-1 were crystallized. In agreement with dimerization of ICAM-1 on the cell surface, a dimer model was postulated (Casasnovas, 1998), allowing dimeric display of the GNWTWP motif. This supports our hypothesis that multimeric display of the motif is essential for high affinity binding. Based on the present findings, we propose that ICAM-1 interacts with p150 via the motif located right upstream of the start of the fifth IG domain. Clearly, further experiments have to be performed to elucidate whether this is indeed the binding epitope.

In conclusion, we have identified a peptide ligand, C-GRWSGWPADL-C binding specifically with high affinity to β 2 integrin p150. Binding of C-GRWSGWPADL-C is not interfering with binding of antibody 4G1 or fibrinogen. The similarity of the peptide sequence of this motif with residues GNWTWP in ICAM-1 suggests that this sequence in ICAM-1 mediates interaction with p150. In future experiments, the potential role of residues GNWTWP in ICAM-1 for interaction with p150 should be investigated. The corresponding interacting motif or a multimeric display of peptide C-GRWSGWPADL-C may serve as potential PMN migration blockers. ICAM-1 is known to play a crucial role in neutrophil (PMN) transendothelial migration as well as in transepithelial transmigration after cytokine stimulation or bacterial exposure (Jaye and Parkos, 2000). Moreover, a multimeric display of peptide C-GRWSGWPADL-C could prove useful for the development of vectors targeting p150 in monocytes or leukocytes from patients

suffering from Hairy Cell Leukemia (HCL) express high levels of p150. Peptide ligands can be used to target p150 positive cells. C-GRWSGWPADL-C might also be helpful to study the function of p150 as well as of ICAM-1.

Acknowledgement

This work was supported by grants to A.O. from the Clöetta Research Foundation and from the Swiss National Science Foundation (No 3100AO-100060). We thank Dr. Ursula Hinz, SwissProt, Geneva, for helpful discussion on the manuscript.

Abbreviations

p150, CD11c/CD18; Mac-1, CD11b/CD18; BSA, bovine serum albumin; TU, transducing units

Key words: integrin, p150, Mac-1, phage-display

Figure legends

Figure 1

Binding of selected phage relative to control phage F2 to purified Mac-1 (A) and p150 (B). Purified integrins coated to polysorb strips were incubated with 10^8 transducing units (TU) of various purified phage (see Table I). After intense washing, phage were eluted with low pH. Recovered phage were titered. A negative control showing binding of C-GRWSGWPADL-C phage to polysorb strips in the absence of integrins is indicated by No. Binding of F2 control phage was normalized to 1. Data represent mean \pm SD of the number of phage plaques on lawns of bacterial cells, determined from three independent experiments.

Figure 2

Binding of purified C-GRWSGWPADL-C phage to p150 in the presence of various concentration of Fibrinogen. ■ C-GRWSGWPADL-C phage □ unspecific phage.

Wells coated with p150 were blocked with heat inactivated BSA to prevent unspecific binding and incubated with various concentrations of fibrinogen for 10 min. C-GRWSGWPADL-C phage (10^8 TU) was then added, followed by incubation for 2 hours. After extensive washing phage were eluted with low pH and titered.

Figure 3

Binding of fibrinogen (A) and synthetic peptide C-GRWSGWPADL-C (B) to purified p150 measured with Surface Plasmon Resonance. P150 was coated on a CM5 BIAcore chip. Various concentrations of fibrinogen and synthetic peptide C-GRWSGWPADL-C were applied. A curve indicating typical receptor-ligand binding was observed. A K_D for fibrinogen of 20 nM and for synthetic peptide C-GRWSGWPADL-C of 20-50 μ M was calculated using BIAevaluation software.

Figure 4

Pattern of binding of C-GRWSGWPADL-C phage and control phage to monocytes and lymphocytes. Monocytes ■ and lymphocytes ■ were isolated from healthy volunteers and binding of control phage (A) and C-GRWSGWPADL-C phage (B) was analyzed in flow cytometric analyses. Cell bound phage were detected with biotinylated anti-M13 phage antibody followed by secondary antibody PE-streptavidin.

Figure 5

C-GRWSGWPADL-C phage binding to monocytes ■ and subset of lymphocytes ■ was investigated in the presence of antibody 4G1 (A) a functional blocker for p150, and control antibody anti-CD14 (B). Simultaneous incubation of antibody 4G1 and C-GRWSGWPADL-C phage (C) or control antibody anti-CD14 and C-GRWSGWPADL-C phage (D).

Figure 6

Alignment of C-GRWSGWPADL-C phage and human ICAM-1 (amino acid 361 - 479). N412 indicates the begin of the fifth domain of ICAM-1. Suggested disulfide bridge between C419 and C457 by SwissProt. Based on the similarity to the sequence of the C-GRWSGWPADL-C phage, we postulate a disulfide bridge between C403 and C419 which would allow a circular display of the clasped sequence similar to that in the phage.

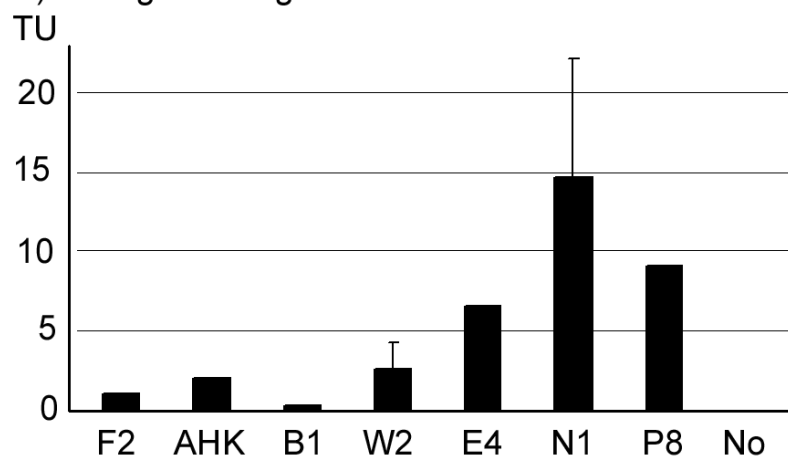
Table 1

Phage selected from pannings on Mac-1(A)and p150(B)

A)	Exp1	B1:	MDKTH FVNE	linear	LL9	EDTA	
		B2:	KQYG MDKLH	linear	LL9	EDTA	
		B3:	MD NGTKRRL	linear	LL9	EDTA	
		B4:	RIF S DKHPP	linear	LL9	EDTA	
	Exp2	E4:	OGGE WRS KAK	circular	CL10	CBRM1/29	
		E5:	TGQLA WRS RD	circular	CL10	CBRM1/29	
		E6:	KHD WQ S PFGE	circular	CL10	CBRM1/29	
	Exp3	AHK:	AHKSARKTE	linear	LL9*	EDTA	
		W2:	WSYWETVAK	linear	LL9*	EDTA	
	B)	Exp4	N1:	GRWSGWPADL	circular	CL10	low pH
		Exp5	P8:	HKGHDRGKKR	circular	CL10	low pH

The linear nonapeptide phage-display library LL9 and the circular decapeptide library CL10 were screened on purified Mac1 (A) or purified p150 (B) as described under “Materials and Methods”. Individual phage clones were selected after 4 or 5 rounds of panning and the sequence of the displayed peptide was determined.

A) Phage binding to Mac1



B) Phage binding to p150

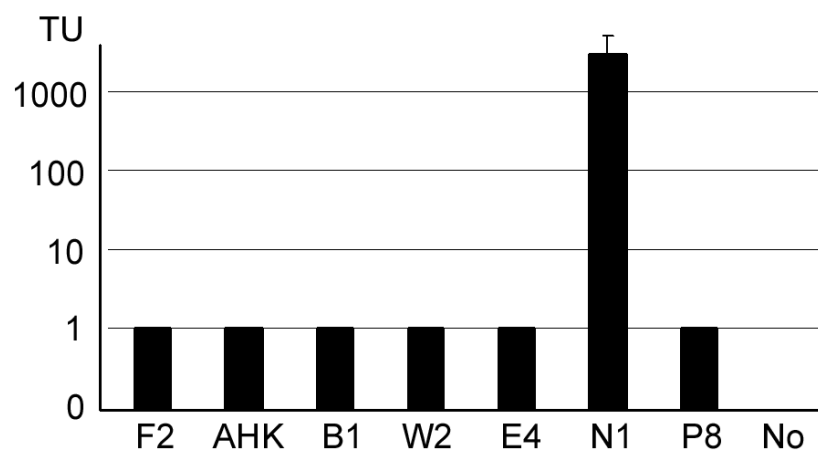


Figure 1

Phage binding in presence of Fibrinogen

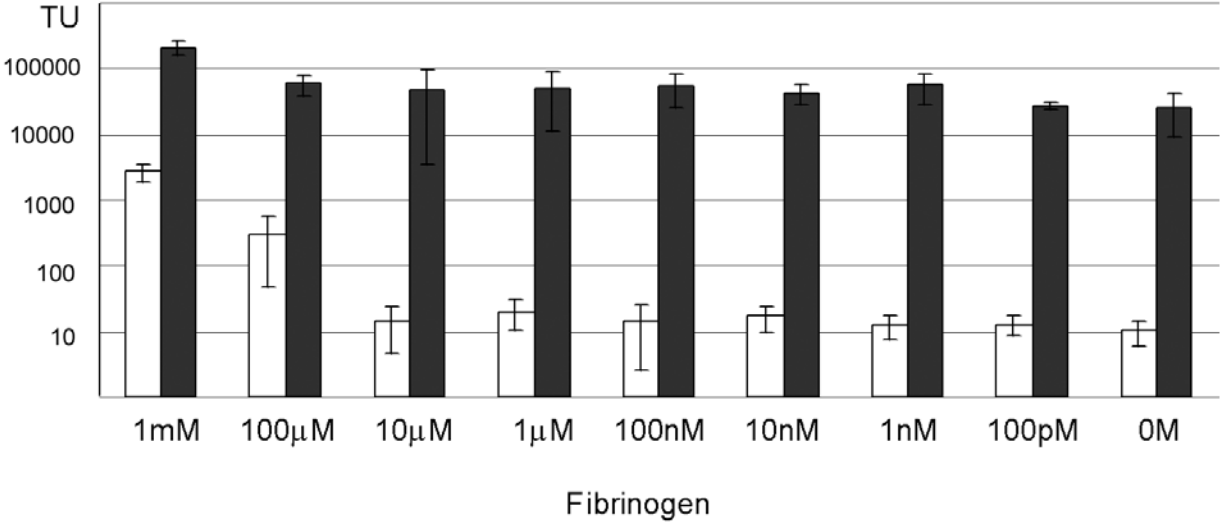


Figure 2

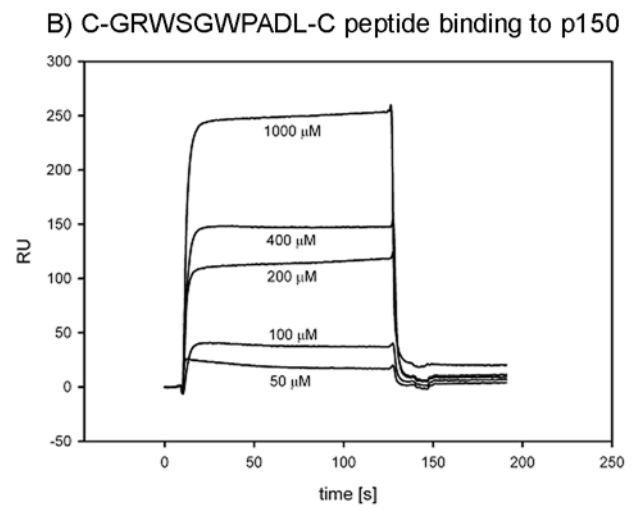
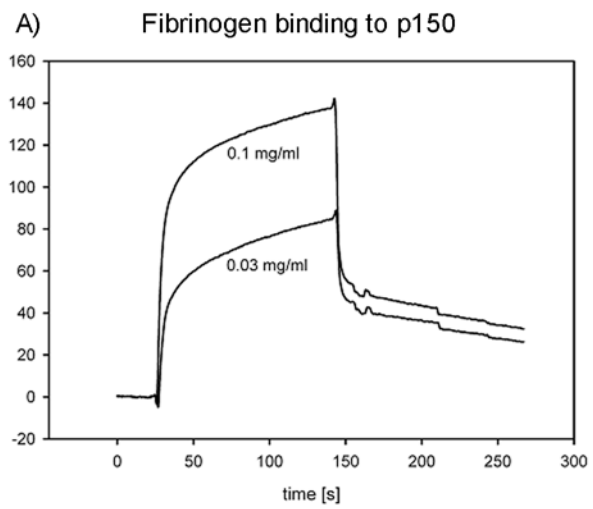


Figure 3

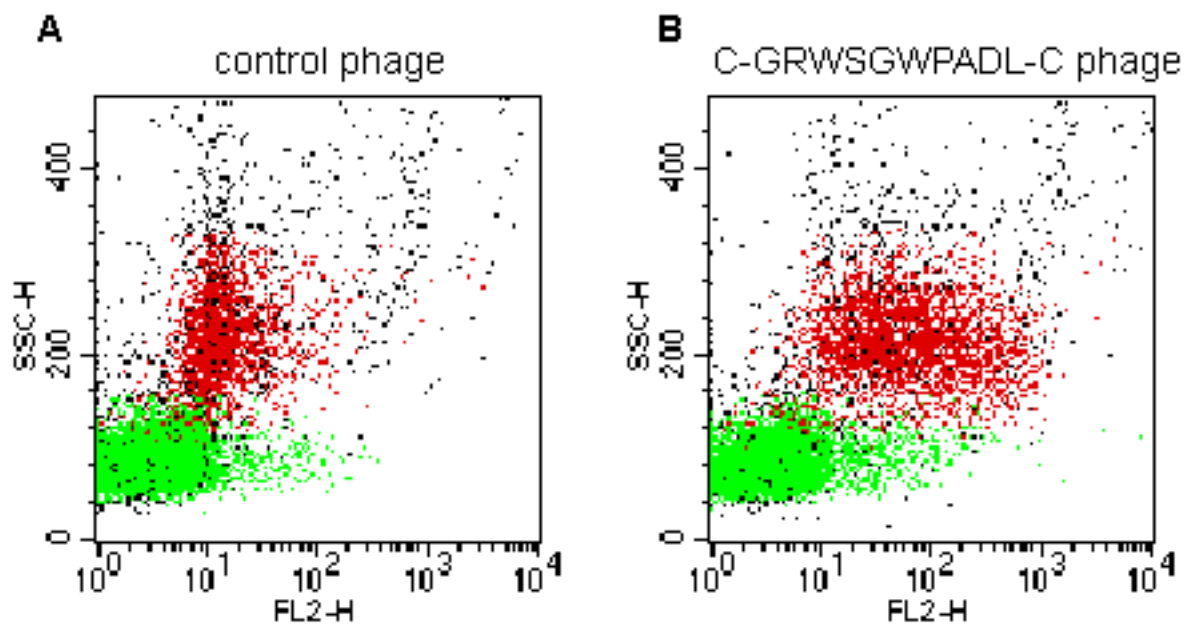


Figure 4

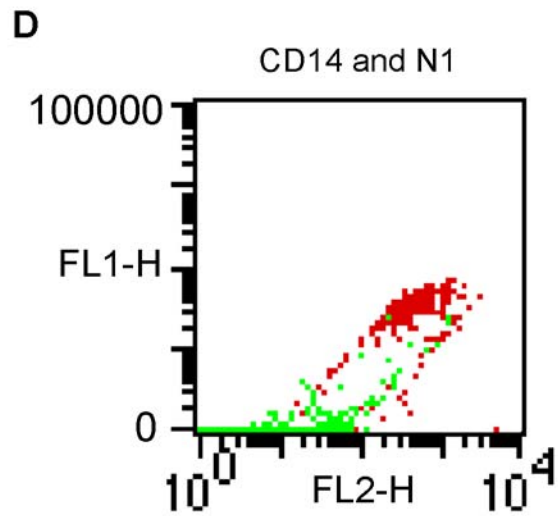
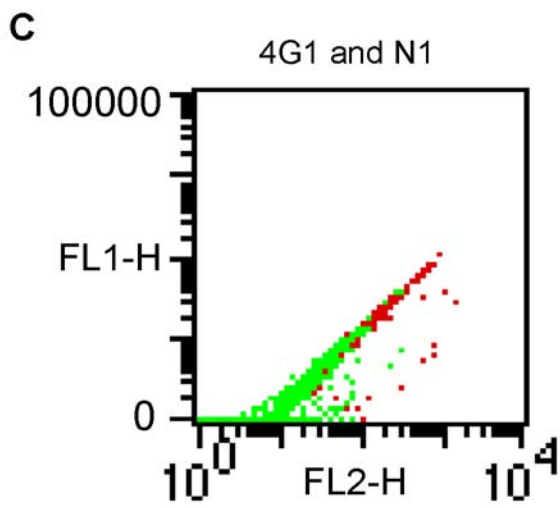
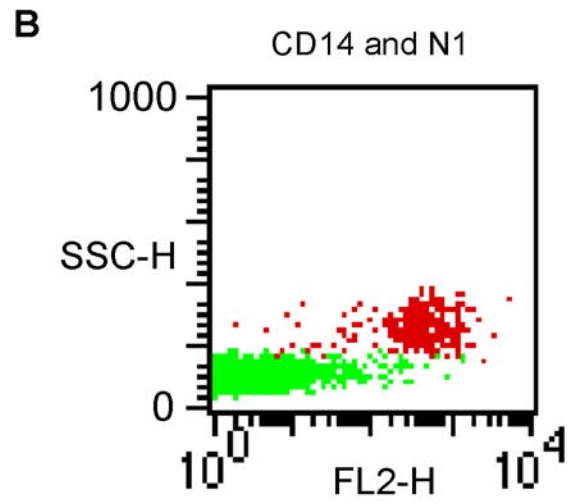
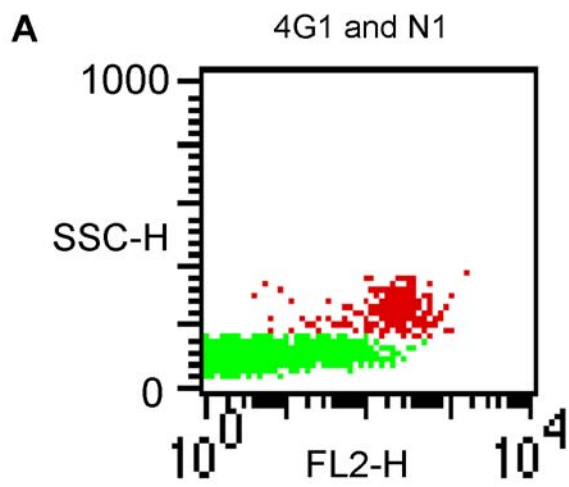


Figure 5

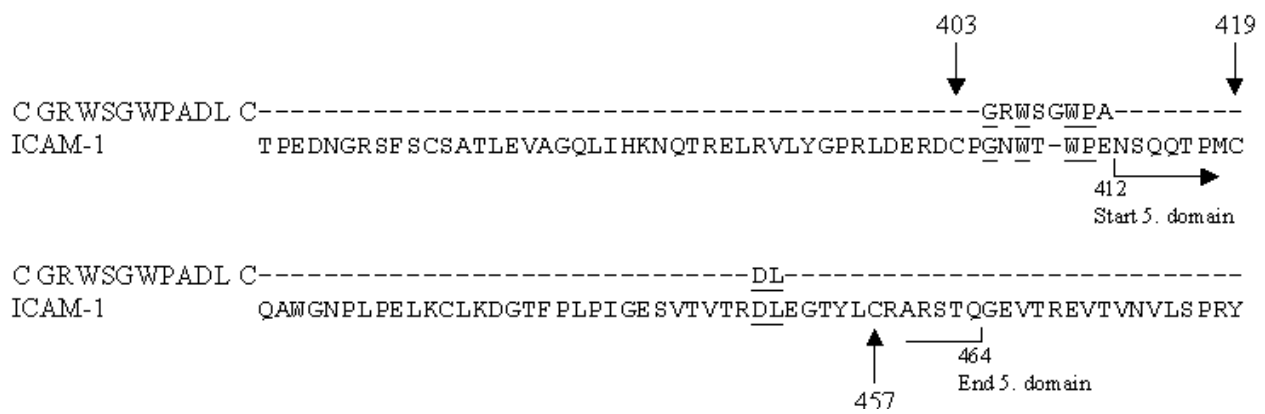


Figure 6

4. References

1. Harris, E.S., et al., *The leukocyte integrins*. J Biol Chem, 2000. **275**(31): p. 23409-12.
2. Casasnovas, J.M., et al., *A dimeric crystal structure for the N-terminal two domains of intercellular adhesion molecule-1*. Proc Natl Acad Sci U S A, 1998. **95**(8): p. 4134-9.
3. Humphries, M.J., *Integrin structure*. Biochem Soc Trans, 2000. **28**(4): p. 311-39.
4. Humphries, M.J., *Insights into integrin-ligand binding and activation from the first crystal structure*. Arthritis Res, 2002. **4 Suppl 3**: p. S69-78.
5. Hughes, P.E., et al., *Breaking the integrin hinge. A defined structural constraint regulates integrin signaling*. J Biol Chem, 1996. **271**(12): p. 6571-4.
6. Qu, A. and D.J. Leahy, *Crystal structure of the I-domain from the CD11a/CD18 (LFA-1, alpha L beta 2) integrin*. Proc Natl Acad Sci U S A, 1995. **92**(22): p. 10277-81.
7. Keizer, G.D., et al., *Membrane glycoprotein p150,95 of human cytotoxic T cell clone is involved in conjugate formation with target cells*. J Immunol, 1987. **138**(10): p. 3130-6.
8. Noti, J.D. and B.C. Reinemann, *The leukocyte integrin gene CD11c is transcriptionally regulated during monocyte differentiation*. Mol Immunol, 1995. **32**(5): p. 361-9.
9. Vorup-Jensen, T., et al., *Structure and allosteric regulation of the alpha X beta 2 integrin I domain*. Proc Natl Acad Sci U S A, 2003. **100**(4): p. 1873-8.
10. Shortman, K. and Y.J. Liu, *Mouse and human dendritic cell subtypes*. Nat Rev Immunol, 2002. **2**(3): p. 151-61.
11. Hynes, R.O., et al., *The diverse roles of integrins and their ligands in angiogenesis*. Cold Spring Harb Symp Quant Biol, 2002. **67**: p. 143-53.
12. Anderson, D.C. and T.A. Springer, *Leukocyte adhesion deficiency: an inherited defect in the Mac-1, LFA-1, and p150,95 glycoproteins*. Annu Rev Med, 1987. **38**: p. 175-94.
13. Jaye, D.L. and C.A. Parkos, *Neutrophil migration across intestinal epithelium*. Ann N Y Acad Sci, 2000. **915**: p. 151-61.
14. Languino, L.R., et al., *Fibrinogen mediates leukocyte adhesion to vascular endothelium through an ICAM-1-dependent pathway*. Cell, 1993. **73**(7): p. 1423-34.
15. Greve, J.M., et al., *The major human rhinovirus receptor is ICAM-1*. Cell, 1989. **56**(5): p. 839-47.
16. Berendt, A.R., et al., *Intercellular adhesion molecule-1 is an endothelial cell adhesion receptor for Plasmodium falciparum*. Nature, 1989. **341**(6237): p. 57-9.
17. Diamond, M.S., et al., *The I domain is a major recognition site on the leukocyte integrin Mac-1 (CD11b/CD18) for four distinct adhesion ligands*. J Cell Biol, 1993. **120**(4): p. 1031-43.
18. Stanley, P., et al., *The second domain of intercellular adhesion molecule-1 (ICAM-1) maintains the structural integrity of the leucocyte function-associated*

- antigen-1 (LFA-1) ligand-binding site in the first domain.* Biochem J, 2000. **351**(Pt 1): p. 79-86.
19. Nham, S.U., *Characteristics of fibrinogen binding to the domain of CD11c, an alpha subunit of p150,95.* Biochem Biophys Res Commun, 1999. **264**(3): p. 630-4.
 20. Lee, M.E., K.J. Rhee, and S.U. Nham, *Fragment E derived from both fibrin and fibrinogen stimulates interleukin-6 production in rat peritoneal macrophages.* Mol Cells, 1999. **9**(1): p. 7-13.
 21. Stacker, S.A. and T.A. Springer, *Leukocyte integrin P150,95 (CD11c/CD18) functions as an adhesion molecule binding to a counter-receptor on stimulated endothelium.* J Immunol, 1991. **146**(2): p. 648-55.
 22. Mazzucchelli, L., et al., *Cell-specific peptide binding by human neutrophils.* Blood, 1999. **93**(5): p. 1738-48.
 23. Yalamanchili, P., et al., *Folding and function of I domain-deleted Mac-1 and lymphocyte function-associated antigen-1.* J Biol Chem, 2000. **275**(29): p. 21877-82.
 24. Koivunen, E., B. Wang, and E. Ruoslahti, *Phage libraries displaying cyclic peptides with different ring sizes: ligand specificities of the RGD-directed integrins.* Biotechnology (N Y), 1995. **13**(3): p. 265-70.
 25. Koivunen, E., et al., *Inhibition of beta(2) integrin-mediated leukocyte cell adhesion by leucine-leucine-glycine motif-containing peptides.* J Cell Biol, 2001. **153**(5): p. 905-16.
 26. Audige, A., et al., *Selection of peptide ligands binding to the basolateral cell surface of proximal convoluted tubules.* Kidney Int, 2002. **61**(1): p. 342-8.
 27. Odermatt, A., et al., *Identification of receptor ligands by screening phage-display peptide libraries ex vivo on microdissected kidney tubules.* J Am Soc Nephrol, 2001. **12**(2): p. 308-16.
 28. Jaye, D.L., et al., *Novel G protein-coupled responses in leukocytes elicited by a chemotactic bacteriophage displaying a cell type-selective binding peptide.* J Immunol, 2001. **166**(12): p. 7250-9.
 29. Jaye, D.L., et al., *Use of real-time polymerase chain reaction to identify cell- and tissue-type-selective peptides by phage display.* Am J Pathol, 2003. **162**(5): p. 1419-29.

Selection of peptide ligands binding to the basolateral cell surface of proximal convoluted tubules

ANNETTE AUDIGÉ, CHRISTOPH FRICK, FELIX J. FREY, LUCA MAZZUCHELLI, and ALEX ODERMATT

Division of Nephrology and Hypertension, Department of Clinical Research, and Institute of Pathology, University of Berne, Berne, Switzerland

Selection of peptide ligands binding to the basolateral cell surface of proximal convoluted tubules.

Background. Recently, we have reported a novel approach of screening phage-display peptide libraries on microdissected intact renal tubular segments and identified an RGD-containing peptide ligand that specifically binds to the basolateral membrane of cortical collecting ducts (CCD). However, screening phage libraries on proximal convoluted tubules (PCT) did not yield a tubule segment-specific ligand. Here, we describe the successful modification of our previously developed phage-display approach and the identification of two distinct ligands that bind specifically to receptors expressed at the basolateral membrane of PCT.

Methods. Ex vivo screening of phage-display peptide libraries for specific ligands was adapted for PCT. The previously developed method was significantly extended by applying it to a distinct tubular segment, varying the number of rounds of biopanning and incubating phage libraries with absorber cells prior to biopanning. Binding specificity and cellular localization of selected peptide-displaying phage or the corresponding synthetic peptide were analyzed using various epithelial cell lines as well as competition assays and confocal immunofluorescence microscopy.

Results. Screening phage-display peptide libraries, depleted of ligands binding to ubiquitously expressed receptors by preincubation with HEK-293 cells, led to the identification of two PCT-specific ligands. Phage expressing peptides with the consensus sequence GV(K/R)GX₃(T/S) or RDXR mediated 15-fold and 13-fold higher binding to PCT than control phage, and binding to PCT was 13-fold and 21-fold higher than binding to CCD, respectively. Neither phage mediated significant binding to various epithelial cell lines, and binding of both ligands was abolished by the addition of the corresponding synthetic peptide. Immunofluorescence experiments revealed a submembrane localization of both ligands upon incubation with PCT.

Conclusions. Exploiting the versatility of phage-display and biopanning allowed the identification of two distinct peptide ligands that bind specifically to the basolateral membrane of PCT. Tubule segment-specific ligands, such as the described

PCT ligands, may be useful for the analysis of cell-extracellular matrix interactions and may contribute to the development of new therapeutic strategies for renal diseases.

Proximal tubules express numerous transporters, channels, and receptors at the luminal and basolateral membrane for the reabsorption of electrolytes, water, amino acids and substances like glucose from the tubular fluid. While many investigators have studied the expression of apically located membrane proteins in proximal tubules [1], little is known about basolateral epithelial markers and their ligands in this segment. Since the expression of cell surface receptors may be significantly altered upon culturing of cells [2, 3], a native system for the identification of kidney tubule-specific ligands is advantageous.

Recently, we described the screening of phage-display peptide libraries ex vivo on microdissected intact renal tubular segments [4]. This approach allowed the identification and characterization of a ligand that binds specifically to cortical collecting duct (CCD), whereas peptides selected from proximal convoluted tubule (PCT) were not tubule segment-specific. Here, we report the successful selection of two ligands that mediate preferential binding to PCT after biopanning phage-display peptide libraries that were pretreated with absorber cells to remove unspecific phage.

METHODS

Sprague-Dawley rat kidneys were perfused in situ via the abdominal aorta, and tubular segments were isolated by microdissection as described recently [4], with minor modifications. The slightly modified perfusion solution contained 120 mmol/L NaCl, 5 mmol/L KCl, 0.25 mmol/L CaCl₂, 1 mmol/L MgSO₄, 0.2 mmol/L Na₂HPO₄, 0.15 mmol/L NaH₂PO₄, 5 mmol/L glucose, 2 mmol/L lactate, 1 mmol/L pyruvate, 4 mmol/L essential and non-essential amino acids, 20 mmol/L HEPES, pH 7.4, and the osmolarity was adjusted to 400 mOsm/kg by the

Key words: phage display, peptide ligands, proximal convoluted tubule, cortical collecting duct, microdissection, basolateral membrane.

Received for publication May 17, 2001

and in revised form July 9, 2001

Accepted for publication August 27, 2001

© 2002 by the International Society of Nephrology

addition of mannitol. The left kidney was treated with perfusion solution containing 3.0 mg/mL (0.9 U/mg) of collagenase Clostridium histolyticum (Serva, Heidelberg, Germany). For the removal of endothelial cells and extracellular matrix, small cortical pieces were incubated in perfusion solution containing 0.65 mg/mL collagenase for approximately 45 minutes at 31°C, and PCT and CCD were microdissected in aerated perfusion buffer containing 0.25 mmol/L CaCl₂ and 1 mg/mL bovine serum albumin (BSA) at 0°C to 4°C. Intact nephron segments of a total length of 25 or 50 mm, corresponding to approximately 7500 and 15000 cells, respectively, were subjected to incubation with phage or synthetic peptides as described below.

Microdissected intact PCT of a total length of 50 mm (15,000 cells) were preincubated in 200 µL of phage incubation buffer (perfusion solution containing 1% BSA and 100 µmol/L chloroquine) for 15 minutes at 37°C. Tubules were then incubated for 40 minutes at 37°C with 10¹⁰ plaque forming units (PFU) of phage from the linear random nonapeptide library LL9 or the circular random decapeptide library CL10 in a first set of biopanning experiments or from depleted LL9 libraries (discussed later in this article in a second set of experiments). The ratio of phage per cell was 6.7×10^5 . Unbound phage was removed by extensive washing, followed by an acid wash and neutralization with perfusion solution. PCT-associated phages were then recovered and amplified as described previously [4]. In subsequent rounds of biopanning, 10¹⁰ PFU of purified selected phage were reapplied to freshly isolated PCT (50 mm, 15,000 cells), and after three or four rounds individual phage clones were isolated and the sequences of the expressed peptides determined.

In an attempt to deplete library LL9 [5, 6] of phage binding to various types of renal tubular segments, two different conditions were chosen. In one set of experiments, 10¹⁰ PFU of phage from library LL9 were incubated with CCD (50 mm, 15,000 cells) for 30 minutes at 37°C, followed by centrifugation of the tubules at $150 \times g$ for three minutes. The ratio of phage per CCD cell was 6.7×10^5 . Subsequently, the supernatant containing the unbound phage was incubated with isolated PCT, and PCT-binding phage were isolated as described above. This procedure of depleting the phage pool on CCD and selection of phage binding to PCT was repeated four times, followed by analysis of individual phage clones. In a second set of experiments, the depletion of library LL9 was performed with HEK-293 cells. Upon incubation of 10¹⁰ PFU of phage with 5×10^6 HEK-293 cells (ratio of 2×10^3 phage/cell), unbound phage were separated from the cells by filtration through 0.45 µmol/L pore size filters (Millipore, Bedford, MA, USA).

Phage-binding to isolated tubules was quantitated according to the selection procedure described above by

incubating tubules (25 mm) at 37°C for 40 minutes with 10¹⁰ PFU of an individual phage clone. In competition experiments, the selected phage and various concentrations of its corresponding synthetic peptide or a random control peptide with the sequence PSRHIPPQL were incubated simultaneously with tubule segments. After acid wash, cell-associated phages were recovered and quantitated by plaque assay.

The binding specificity of selected PCT-binding ligands was assessed by simultaneous incubation of 10¹⁰ PFU of an individual phage clone with either 10⁵ cells of different epithelial origin (MDCK-II, kidney CCD origin; MCF-7, breast; SUT, lung; SW-620, intestine; HELA, cervix; LLCPK-1, kidney PCT origin; rat GMC, kidney glomerular origin) or the corresponding synthetic peptide (Macromolecular Resources, Fort Collins, CO, USA) at various concentrations (Fig. 1). After extensive washing, cell-associated phage was determined as described above.

For intracellular localization of peptides, microdissected PCT (25 mm) were preincubated in phage incubation buffer (perfusion solution containing 1% BSA and 100 µmol/L chloroquine) for 15 minutes at 37°C prior to the addition of 10 µmol/L of synthetic biotinylated peptide and incubation for one hour at 37°C. Reactions were terminated by adding ice-cold phage incubation buffer, followed by the removal of unbound peptides by extensive washing and acidic wash. The pelleted PCT were taken up in 100 µL of microdissection buffer, subjected to cytospin centrifugation at $100 \times g$ for three minutes onto glass cover slides and fixed with 4% paraformaldehyde supplemented with 4% sucrose in 100 mmol/L sodium phosphate buffer, pH 7.4, for 10 minutes at 25°C. Immunostaining and analysis by confocal microscopy were performed as described previously [4], whereby the Na/HCO₃ cotransporter was detected with a rabbit polyclonal antibody (Chemicon, Temecula, CA, USA) and ALEXA-594-conjugated goat anti-rabbit IgG, and synthetic peptides were visualized using fluorescein-conjugated mouse monoclonal anti-biotin antibody (Molecular Probes, Leiden, The Netherlands).

Statistical analysis of phage binding specificity was performed using the Wilcoxon signed rank test. A *P* value less than 0.05 was considered as statistically significant.

RESULTS

Screening phage display peptide libraries for PCT-binding ligands

In a previous screening of phage-display libraries, four rounds of selection on isolated PCT yielded phage-expressing peptides of the consensus sequence KX₃TNHP, which were not tubule segment-specific. Due to the competitive nature of biopanning, ligands binding to receptors with lower expression levels or ligands with lower affinity may have been lost after four rounds of selection.

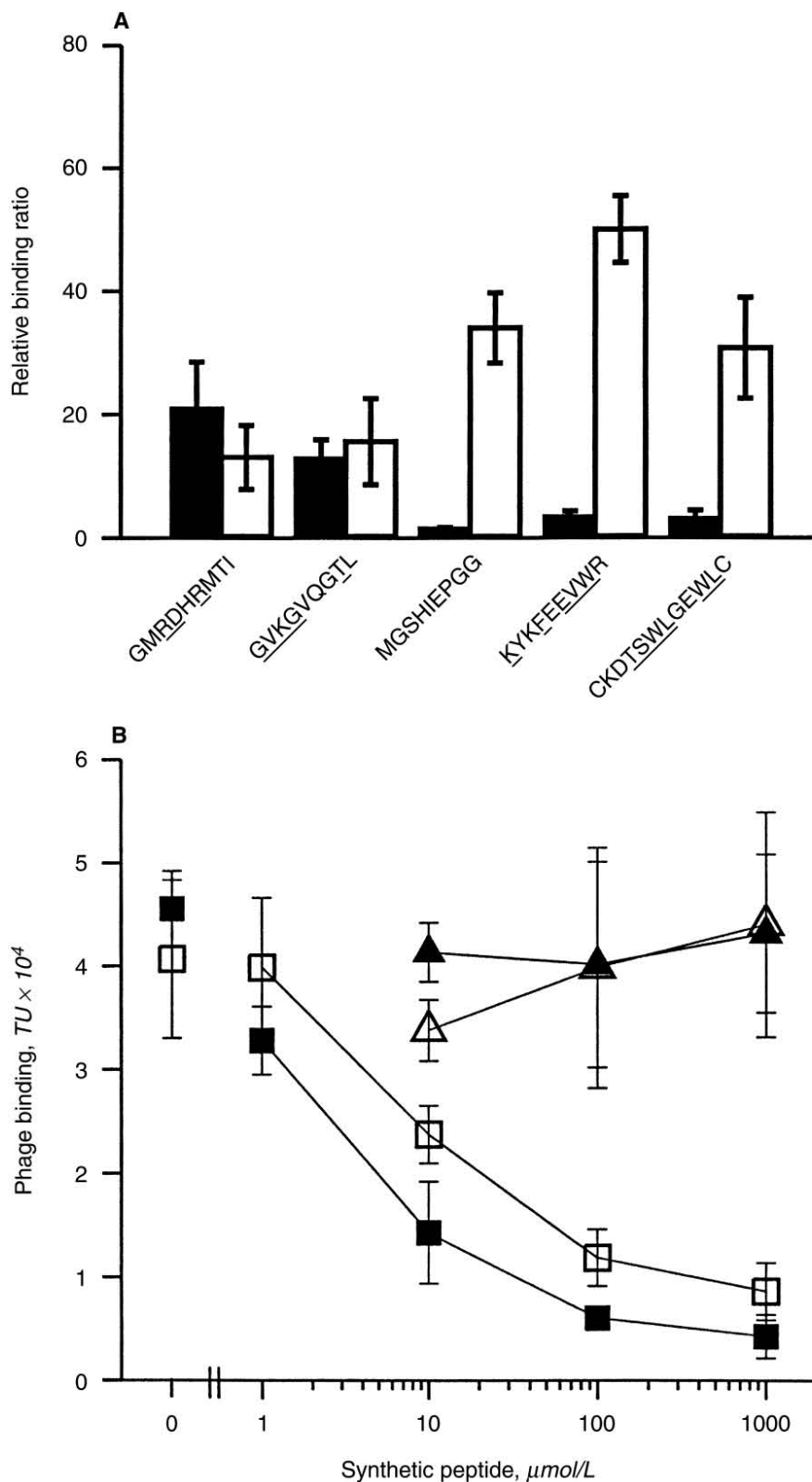


Fig. 1. Analysis of phage-binding specificity. (A) Ratios of phage binding to proximal convoluted tubule (PCT) versus cortical collecting duct (CCD) (PCT/CCD, ■) and of phage binding versus control to PCT [PCT(specific phage)/PCT(control phage); □]. (B) Inhibition of PCT binding of GV-phage by a random control peptide (Δ) or by the synthetic peptide GVKGVQGTI (\square), and inhibition of PCT binding of RD-phage by a random control peptide (\blacktriangle) or by the synthetic peptide GMRDHRMTI (\blacksquare) was determined. Data represent mean \pm SE of the number of phage plaques (A) or of phage binding ($\text{PFU} \times 10^4$) per cm of tubule (B) from three to five independent experiments.

Therefore, in the present study, individual phage clones were analyzed after three rounds of selection on PCT. Phage expressing the consensus sequence $\text{KX}_2\text{FX(E/D)VW}$ were recovered from panning the linear library LL9

in addition to the motif KX_3TNHP (Table 1). Three rounds of biopanning the circular library CL10 yielded the circular motif $\text{C-X}_2(\text{T/S})\text{SWLXEWL-C}$ (Table 1), which mediated 30-fold higher binding to PCT than con-

Table 1. Peptides selected from microdissected proximal convoluted tubules (PCT)

Type of library <i>N</i> of biopanning rounds	Selected sequence	<i>N</i> of identical sequences
Linear Library LL9 (3 rounds, 12 clones were sequenced)	<u>K</u> MGGT <u>NH</u> PE	(2)
	<u>K</u> SAVT <u>NH</u> GI	(2)
Consensus	HLNH <u>PMS</u> IM	(1)
	KXXXXTNHP	
Consensus	<u>K</u> YK <u>F</u> E <u>E</u> VWR	(4)*
	<u>K</u> MA <u>F</u> Q <u>D</u> VWM	(2)
	<u>K</u> S <u>G</u> <u>F</u> NE <u>V</u> WP	(1)
	KXXX <u>F</u> (E/D)W	
Constrained Library CL10 (3 rounds, 8 clones were sequenced)	<u>C</u> KDT <u>S</u> W <u>L</u> GE <u>W</u> LC	(4)*
	<u>C</u> E <u>K</u> SS <u>W</u> LA <u>E</u> WLC	(2)
	<u>C</u> LL <u>T</u> S <u>F</u> LE <u>V</u> YC	(1)
	<u>C</u> LISQRHV <u>A</u> SSC	(1)
Consensus	C(T/S)SWL(A/G)EWLC	
Linear Library LL9 Depleted on CCD	<u>M</u> GSHIE <u>P</u> GG	(4)*
	<u>T</u> G <u>S</u> F <u>G</u> VAGG	(2)
Depleted on CCD (4 rounds, 12 clones were sequenced)	<u>G</u> GM <u>V</u> S <u>Q</u> GSK	(1)
	<u>G</u> GM <u>G</u> EH <u>G</u> SS	(1)
Consensus	G(G/S)XXXXG(G/S)	
Linear Library LL9 Depleted on HEK-293	<u>G</u> VK <u>G</u> VQ <u>G</u> T <u>L</u>	(3)*
	<u>H</u> GVR <u>G</u> N <u>L</u> IS	(2)
Depleted on HEK-293 (4 rounds, 16 clones were sequenced)	<u>G</u> VR <u>G</u> QL <u>A</u> TP	(1)
	GV(K/R)GXXX(T/S)	
Consensus	<u>G</u> MR <u>D</u> HR <u>M</u> TI	(4)*
	<u>E</u> TM <u>Q</u> RD <u>V</u> RA	(2)
	<u>Y</u> RD <u>F</u> RD <u>I</u> WA	(1)
	<u>S</u> LR <u>D</u> RG <u>F</u> T	(1)
	<u>H</u> LN <u>M</u> W <u>R</u> D <u>G</u> G	(1)
	<u>G</u> GA <u>I</u> K <u>D</u> T <u>Q</u> N	(1)
	RDXR	

Alignment of phage-displayed peptides isolated from screening the linear nonapeptide library LL9 or the circular decapeptide library CL10 on microdissected PCT. To deplete library LL9 of ubiquitously binding phage, a library aliquot was incubated with either CCD or HEK-293 cells in each round of biopanning, and the pool of unbound phage was screened for phage binding to PCT. The number of isolated phage expressing identical peptide sequences is indicated in parenthesis. The phage ligands used for analytic studies are indicated by an asterisk. Residues characteristic for the binding motif are underlined.

trol phage ($P < 0.05$; Fig. 1A). Unfortunately, all three ligands selected from screening crude libraries were not tubule segment-specific with only two- or threefold increased binding to PCT compared to CCD (Fig. 1A).

Affinity purification of PCT-specific peptide ligands from depleted libraries

In an attempt to deplete the linear nonapeptide library LL9 of ligands binding unspecifically to different nephron segments, we incubated a library aliquot with isolated CCD prior to panning unbound phage on microdissected PCT. This procedure resulted in the selection of phage expressing peptides with the conserved sequence G(G/S)X₄G(G/S) (Table 1), which was not observed when screening the undepleted library. Binding studies using purified phage expressing the peptide MGSHEPVG revealed 34-fold increased binding to PCT compared to control phage but almost equal binding to PCT and CCD (Fig. 1A).

To achieve a more efficient depletion of ubiquitously binding ligands, a library aliquot was incubated with HEK-293 cells at a ratio of 2×10^3 phage per cell. Comparison of the peptide sequences expressed by 16 isolated individual phage clones revealed the two distinct motifs GV(K/R)GX₃(T/S) (GV-phage) and RDXR (RD-phage) (Table 1).

Neither motif was observed in previous biopanning experiments.

Characterization of binding properties of GV-phage and RD-phage

Analysis of binding of GV-phage or RD-phage to microdissected tubules revealed 15-fold and 13-fold increased binding to PCT versus control phage, whereby binding ratios of PCT to CCD were 13-fold and 21-fold, respectively ($P < 0.05$; Fig. 1A). The binding specificity of GV-phage and RD-phage was characterized further by comparing binding of specific phage with that of control phage to various epithelial cell lines. Binding of both GV-phage and RD-phage to isolated CCD or to the cell lines MDCK-II (kidney, CCD origin), MCF-7 (breast), SUT (lung), SW-620 (colon), HELA (cervix), LLCPK-1 (kidney, PCT origin), and GMC (kidney, glomerular origin) was determined by using the plaque assay as indicated in Figure 1A, yielding binding that was not significantly higher than control phage binding (data not shown). Highest binding of the RD-phage, at only 2.5-fold higher levels than control phage binding, was observed for LLCPK-1 cells. In competition assays, coinci-

segments successfully yielded a ligand binding specifically to CCD, however, no specific ligand was selected for PCT [4]. The aim of the present work was to extend this method in order to make it suitable for the identification of ligands for various defined renal segments such as PCT. For this purpose, the previous screening procedure for PCT was extended by two modifications. First, analysis of individual phage clones was performed after three instead of four rounds of biopanning on PCT. Since the screening of phage-display libraries is a competitive process that ultimately tends to result in the selection of the “best-fit” sequence, ligands binding to receptors with lower expression levels or ligands with lower affinity may have been lost after four rounds of selection in the previous experiments. The reduction of panning rounds resulted in the isolation of two peptide ligands that were not observed previously (Table 1). Their motifs, $KX_2FX(E/D)VW$ and $C-X_2(T/S)SWLXEWL-C$, resemble each other when considering conservative substitutions of amino acids, suggesting that both peptides bind to the same receptor. However, these ligands were again not tubule segment-specific. Second, in order to deplete phage-libraries of ubiquitously binding ligands, phages were preincubated with absorber cells prior to selection on PCT. The number of approximately 1.5×10^4 CCD cells and a ratio of 6.7×10^5 phages per cell might have been insufficient for library depletion, leading to the isolation of a peptide ligand with the conserved sequence $G(G/S)X_4G(G/S)$ (Table 1) that bound to PCT but was not segment specific (Fig. 1A). In contrast, efficient depletion of unspecific phage was achieved by incubation of phage with HEK-293 cells at a ratio of 2×10^3 phages per cell. This modification allowed the isolation of two distinct phage containing the motifs $GV(K/R)GX_3(T/S)$ and $RDXR$ (Table 1) which exhibited significant binding specificity for PCT over CCD (Fig. 1A). A database search with the consensus sequences of the two motifs did not reveal their native epitope. However, possible candidates among several proteins containing the motif $GV(K/R)GX_3(T/S)$ are collagen- α subunits. Human and rat collagen $\alpha 1$ (III) contain the sequence $GVKGERGS$ whereas human collagen $\alpha 1$ (XI) and collagen $\alpha 1$ (XVI) contain the sequence $GVRGLLKGS$ and $GVRGLPGT$, respectively. It should be noted here that none of the ligands selected from PCT contained an RGD sequence as previously found in panning experiments on isolated CCD [4]. Further analysis of binding specificity of these two phage to various epithelial cell lines revealed binding that was less than 2.5-fold that of control phage (data not shown). Importantly, the two motifs did not mediate significant binding to LLCPK-1 cells, which are often used as a cell model for PCT. Isolation and culturing of rat proximal tubule cells have been shown to result in significantly altered expression and distribution of cell surface receptors [2]. These observations emphasize the

need for a native cell system for the identification of renal epithelial cell ligands and their cognate receptors.

Detection of GV-peptide and RD-peptide by immunofluorescence suggested the initial binding of the specific peptides to the basolateral cell surface (not shown) and internalization to a submembranous localization upon prolonged incubation at 37°C (Fig. 2). Evidence for internalization also is given by the fact that phage resisted the acid wash after incubation with PCT for 40 minutes at 37°C. The submembranous localization of specific peptides may be explained by a recycling pathway between the cell membrane and early endosomes as described for some receptor-ligand complexes [7]. Alternatively, further trafficking of the PCT-binding peptides beyond early endosomes may have been hampered by a disruption of the cellular microtubule network due to a lack of oxygen or a temperature-dependent effect. Actin filaments and microtubules are involved in endo- and exocytotic pathways, whereby endocytosis from the apical membrane appears to be more affected by cytoskeleton disrupting agents than from basolateral membranes [8, 9]. In proximal tubule cells, ischemia causes a rapid, duration-dependent dissociation of the actin cytoskeleton and a redistribution of some surface membrane proteins [10]. Cold treatment followed by rewarming of renal epithelial cells results in a partially reversible disruption of the microtubule network, especially in proximal tubules, and a redistribution of some membrane proteins [11]. We cannot exclude the possibility that in our experiments microtubules were affected by the microdissection procedure that was performed on ice and did not completely recover within the 15-minute adaption period at 37°C prior to the addition of peptide ligands.

The utility of defining basolateral ligands for PCT is twofold. Such ligands are relevant for putative investigations of cell-matrix interactions and for therapeutic purposes. Delivery of biologically active molecules to the proximal tubule is of interest in some acquired or congenital proximal tubulopathies such as Dent's disease [12] or Fanconi syndrome [13]. Ligands such as those found in the present study may be used for targeting of viral or non-viral vectors to distinct nephron segments. Transduction of renal epithelial cells via the basolateral membrane, however, necessitates the access of the delivery vector from the blood stream across the endothelium and the extracellular matrix to the epithelium, a pathway shown by other groups to be facilitated by coapplication of substances that increase vascular permeability [14].

In conclusion, we have significantly extended our recently developed strategy of screening phage-display libraries *ex vivo* on microdissected renal tubular segments and identified two peptide ligands that bind specifically to the basolateral cell surface of PCT. The identification and characterization of ligands with tubule segment-specific properties provide a means to extend existing

knowledge about tubular epithelial cell functions such as cell-extracellular matrix interactions and receptor-mediated endocytosis, and contributes to the development of vectors for drug and/or gene delivery to specific renal tubular segments for future therapeutic treatment.

ACKNOWLEDGMENTS

This work was supported by grants from the Swiss National Science Foundation No. 31-59511.99 (A.O.) and No. 31-61505.00 (F.J.F.). We thank Dr. Kurt Baltensperger, Department of Clinical Research, University of Berne, for helpful advice in confocal microscopy.

Reprint requests to Dr. Alex Odermatt, Division of Nephrology and Hypertension, Department of Clinical Research, Freiburgstrasse 15, University of Berne, Berne, Switzerland
E-mail: alex.odermatt@dkfz.unibe.ch

REFERENCES

- CHRISTENSEN EI, BIRN H, VERRON P, et al: Membrane receptors for endocytosis in the renal proximal tubule. *Int Rev Cytol* 180:237-284, 1998
- REBELO L, CARMO-FONSECA M, MOURA TF: Redistribution of microvilli and membrane enzymes in isolated rat proximal tubule cells. *Biol Cell* 74:203-209, 1992
- SHEPPARD D: Epithelial integrins. *Bioessays* 18:655-660, 1996
- ODERMATT A, AUDIGE A, FRICK C, et al: Identification of receptor ligands by screening phage-display peptide libraries ex vivo on microdissected kidney tubules. *J Am Soc Nephrol* 12:308-316, 2001
- MAZZUCHELLI L, BURRITT JB, JESAITIS AJ, et al: Cell-specific peptide binding by human neutrophils. *Blood* 93:1738-1748, 1999
- BURRITT JB, BOND CW, DOSS KW, et al: Filamentous phage display of oligopeptide libraries. *Anal Biochem* 238:1-13, 1996
- KLAUSNER RD, VAN RENSWOUDE J, ASHWELL G, et al: Receptor-mediated endocytosis of transferrin in K562 cells. *J Biol Chem* 258:4715-4724, 1983
- SCHELLING JR, HANSON AS, MARZEC R, et al: Cytoskeleton-dependent endocytosis is required for apical type 1 angiotensin II receptor-mediated phospholipase C activation in cultured rat proximal tubule cells. *J Clin Invest* 90:2472-2480, 1992
- GOTTLIEB TA, IVANOV IE, ADESNIK M, et al: Actin microfilaments play a critical role in endocytosis at the apical but not the basolateral surface of polarized epithelial cells. *J Cell Biol* 120:695-710, 1993
- MOLLITORIS BA, WAGNER MC: Surface membrane polarity of proximal tubular cells: Alterations as a basis for malfunction. *Kidney Int* 49:1592-1597, 1996
- BRETON S, BROWN D: Cold-induced microtubule disruption and relocalization of membrane proteins in kidney epithelial cells. *J Am Soc Nephrol* 9:155-166, 1998
- THAKKER RV: Pathogenesis of Dent's disease and related syndromes of X-linked nephrolithiasis. *Kidney Int* 57:787-793, 2000
- SUN MS, HATTORI S, KUBO S, et al: A mouse model of renal tubular injury of tyrosinemia type 1: Development of de Toni Fanconi syndrome and apoptosis of renal tubular cells in Fah/Hpd double mutant mice. *J Am Soc Nephrol* 11:291-300, 2000
- WANG G, DAVIDSON BL, MELCHERT P, et al: Influence of cell polarity on retrovirus-mediated gene transfer to differentiated human airway epithelia. *J Virol* 72:9818-9826, 1998

Part II

1.	Summary	1
2.	Introduction	2
2.1.	11 β -hydroxysteroid dehydrogenase	2
2.2.	Insertion of newly synthesized proteins into the membrane	5
2.3.	Outlook	6
2.4.	References	7
3.	Manuscripts and Publications	
3.1.	Specific Amino Acid Residues rather than Net Charge Distribution determine the Topology of 11 β -Hydroxysteroid Dehydrogenase Type 1 and the 50-kDa Esterase/Arylacetamide Deacetylase E3	8
4.	Acknowledgement	29
5.	Curriculum vitae	30

1. Summary

11 β -hydroxysteroid dehydrogenase type 1 (11 β -HSD1) converts biologically inactive cortisone into biologically active cortisol. It acts as a reductase and catalyzes the 11-ketogroup of cortisone. 11 β -HSD1 activity was shown to play a critical role in several disease states such as obesity and diabetes type 2. A better understanding of 11 β -HSD1 in terms of structure and function is therefore of interest.

11 β -HSD1 is a single transmembrane endoplasmatic reticulum (ER) membrane protein, having a short N-terminal membrane anchor and the catalytic domain oriented towards the ER-lumen. The physiological role of the 11 β -HSD1 luminal topology is still unclear. Previous studies showed, that a single point mutation of a single positively charged amino acid at the cytoplasmic side of the membrane anchor (Lys5) inverts the topology of the enzyme towards the cytosol. Surprisingly, such mutants retain wild-type like activity.

Here, we show that negatively charged glutamates located on the cytoplasmic side of the membrane anchor also are critical for the topology. In addition these glutamates are critical for the enzyme activity.

The ER membrane anchor of 50 kDa-esterase/arylacetamide deacetylase (E3) has a high homology with the membrane anchor of 11 β -HSD1, but otherwise E3 is functionally not related with 11 β -HSD1. In a previous analysis, changing the topology of E3 by a single point mutation on the cytoplasmic side of the membrane anchor failed. In the present work, we show that mutating negatively charged amino acids into positively charged residues on the luminal side of the transmembrane sequence determines the cytoplasmic orientation of these E3 mutants.

This study clarifies the relevance of negative charges on the luminal side of the membrane anchor of 11 β -HSD1 and E3. Understanding more about the membrane anchor determining the topology of 11 β -HSD1 may help to elucidate the physiological function of the luminal topology in future experiments.

2. Introduction

The adrenal glands are situated above the kidneys. They consist of an outer region or cortex and an inner region called medulla. The cortex produces a class of lipid-soluble hormones derived from cholesterol and called steroids. Cortisol is a steroid hormone and is secreted from the zona fasciculata of the adrenal cortex under the control of adrenocorticotrope-hormones (ACTH). ACTH secretion is controlled by an endocrine negative feedback mechanism, with cortisol inhibiting ACTH production (synthesis). Highest levels of cortisol and ACTH are measured early in the morning and lowest levels around midnight.

Beside glucocorticoids the mineralcorticoids are also synthesized in the adrenal glands, e.g. in the outer zona glomerulosa. The mineralcorticoids are essential for maintenance of sodium and potassium balance and the regulation of the blood pressure.

2.1. 11 β -hydroxysteroid dehydrogenases

Two isoforms of 11 β -hydroxysteroid dehydrogenases (11 β -HSD) are known, called 11 β -hydroxysteroid dehydrogenase type 1 (11 β -HSD1) and 11 β -hydroxysteroid dehydrogenase type 2 (11 β -HSD2).

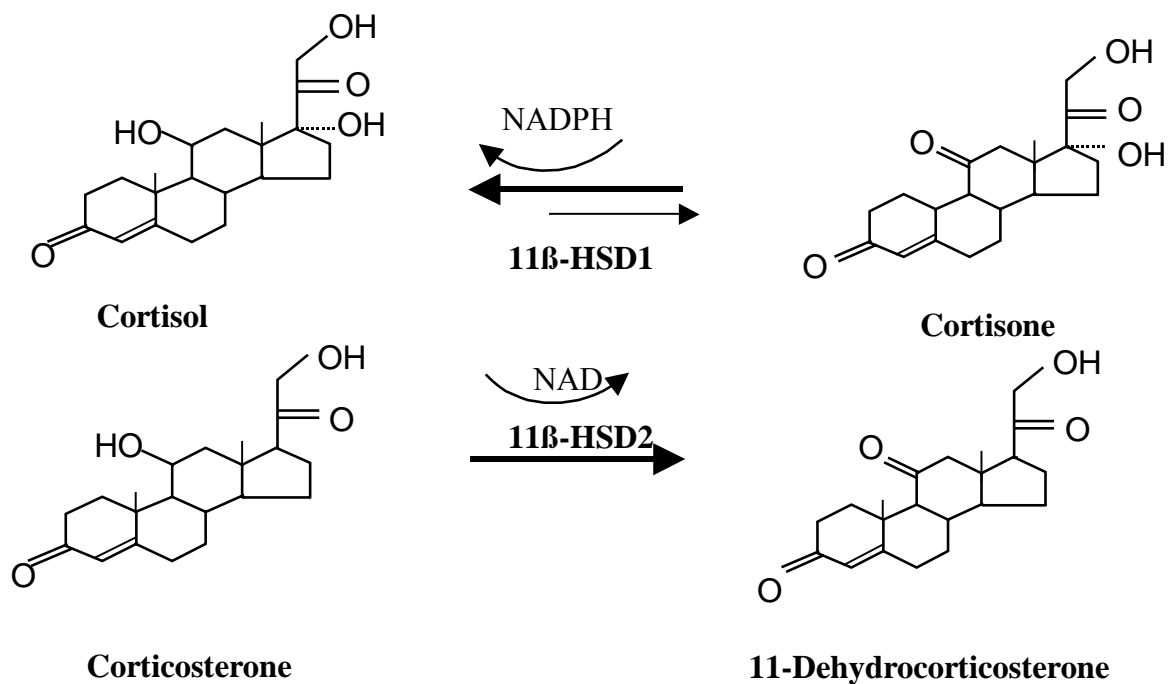


Figure 1

The two isoenzymes 11 β -HSD1 and 11 β -HSD2 interconvert glucocorticoids. Type 1 acts predominantly as a reductase (substrates are cortisone and 11 β -dehydrocorticosterone, the preferred cofactor is NADP(H) in vivo but has oxidative activity (substrates are corticosterone and cortisol, the preferred cofactor is NAD). Type 2 acts exclusively as an oxidase and accepts cortisol and corticosterone as substrates.

They catalyze the interconversion of corticosteroids (cortisol in human and corticosterone in rodents) [1, 2]. Although 11 β -HSD1 is a bidirectional enzyme *in vitro*, it acts *in vivo* predominantly as a reductase and converts the biologically inactive cortisone from its 11-keto form into the biologically active 11 β -hydroxy form cortisol. In contrast 11 β -HSD2 catalyzes exclusively the oxidative reaction from cortisol to cortisone. The two isoenzymes share only 18% identical amino acid sequence and have different physiological roles and tissue-specific expression.

11 β -HSD2 plays an essential role in the protection of the mineralcorticoid receptor from inappropriate activation by glucocorticoids. Mutations in the gene encoding 11 β -HSD2 lead to elevated intracellular concentrations of active 11 β -hydroxyglucocorticoids and, as a consequence, cause excessive activation of the mineralcorticoid receptor [3]. This syndrome is called apparent mineralcorticoid excess since the receptor is no longer controlled by aldosterone but overactivated by cortisol. 11 β -HSD2 knock-out mice develop a similar syndrome of excessive cortisol dependent mineralcorticoid receptor activation with sodium retention and severe hypertension [4]. Recent studies showed the cytoplasmic orientation of 11 β -HSD2, which is an integral ER membrane protein [5, 6]. The cytoplasmic orientation is important for the efficient protection of the mineralcorticoid receptor from cortisol.

11 β -HSD1 regulates the local activation of glucocorticoid hormones in tissues like liver and adipose tissue and is thereby a key regulator of tissue concentrations of cortisol. Animals overexpressing selectively the 11 β -HSD1 gene in adipose tissue convert increased amounts of cortisone to cortisol but have normal glucocorticoid levels in plasma. The transgenic mice develop visceral obesity, hyperglycemia and become insulin-resistant [7]. In contrast, knockout 11 β -HSD1 animals have normal glucocorticoid levels in the plasma, but cannot regenerate glucocorticoid within cells in liver and adipose tissue and are thereby protected from visceral obesity and insulin resistance [4].

Agarwal et al first described the cloning of rat liver 11 β -HSD in 1989 [8]. 11 β -HSD from rat liver. Two years later the human 11 β -HSD1 was cloned [9]. The gene is located on chromosome 1 and contains six exons. 11 β -HSD1 belongs to the short-chain alcohol dehydrogenase (SCAD) superfamily, also known as short-chain dehydrogenases/reductases (SDR). The SDR belong to the superfamily of Rossmann-fold proteins (RFP). The RFP, which bind NAD or NADP use a structurally equivalent and evolutionary conserved cofactor-binding site and they interact with the adenosine and ribose moieties of the cofactor in a very similar manner [10]. The second characteristic feature of this enzyme class is the conserved inner surface of a α -helix in which a tyrosine side chain is positioned in close proximity to a lysine residue four residues downstream in the sequence. The main function of this Tyr-Lys couple is to facilitate tyrosine hydroxyl group participation in proton transfer [11].

11 β -HSD1 is a 34 kDa protein (292 amino acids) and is an integral membrane protein with restricted localization to the endoplasmatic reticulum (ER) membrane [5, 12]. The protein has a hydrophobic N-

terminal sequence with a single transmembrane span, which acts as an anchor and determines restricted localization to the ER-membrane. 11 β -HSD1 belongs to the type 2 transmembrane proteins having an N-terminal stop sequence towards the cytosol and the C-terminal catalytic domain, protruding into the ER-lumen. 11 β -HSD1 contains three glycosylation sites at positions Asn¹²³, Asn¹⁶² and Asn²⁰⁷, respectively. Partial inhibition of glycosylation of 11 β -HSD1 did not affect the reductase activity, but decreased the dehydrogenase activity 50% [13]. Other studies did not find altered activities after inhibition of glycosylation [14-16]. The K_m of 11 β -HSD1 for the oxidase reaction and reductase reactions are in the high nanomolar to low micromolar range. Despite of the importance of 11 β -HSD1 and its role in disease relatively little is known on the structure function relationship and the physiological role for the orientation of 11 β -HSD1 to the ER-lumen remains unclear.

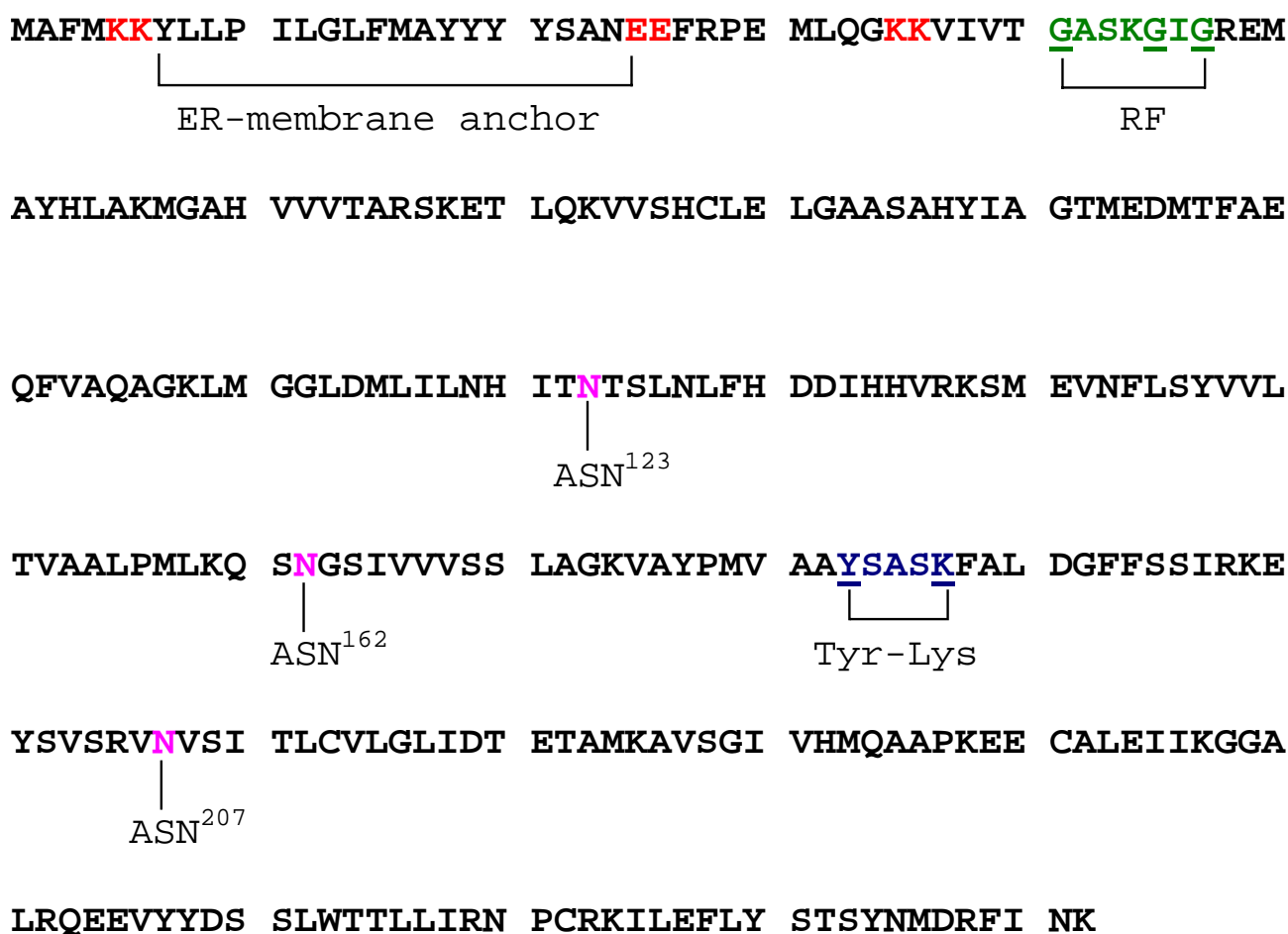


Figure 2

Features and amino acid sequence of 11 β -HSD1, conserved sequences in motifs are underlined

- amino acids which were mutated in the present study
- glycosylation sites
- Rossmann-fold (RF) protein binding the cofactor NADP(H)
- Tyr-Lys motif, catalytic center, (CC)

2.2. Insertion of newly synthesized proteins into the membrane

ER membrane proteins are distinguished concerning their orientation and the number of transmembrane domains. Type 1 proteins have a signal sequence on the amino terminus, which enters first through the translocating channel until a hydrophobic stop sequence is reached. The hydrophobic stop sequence is then inserted into the membrane and forms the anchor for that protein. The signal sequence at the N-terminus is then cleaved by a protease located inside the ER-lumen. Type 2 proteins differ from Type 1 proteins that they do not have a cleavable signal sequence and that they have a rather long hydrophobic region that mediates anchoring in the membrane. Type 3 proteins differ from Type 1 and 2 proteins that they do not have a cleavable signal sequence and that they have a rather long hydrophobic region that mediates anchoring in the membrane.

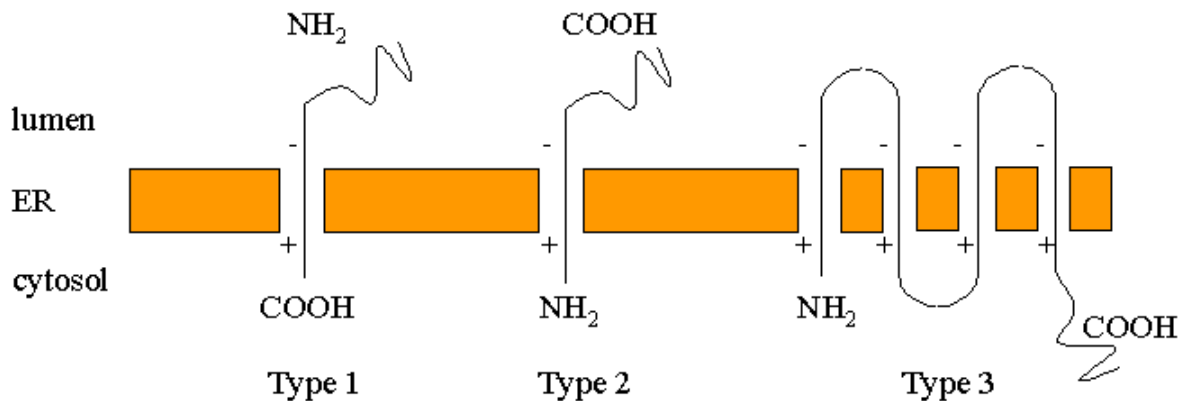


Figure 3

Topology of integral membrane proteins Type 1, having the N-terminus on the trans-side of the membrane (luminal), Type 2, having the N-terminus on the cis-side of the membrane (cytoplasmic) and Type 3, with two or more membrane spanning segments. Type 1 and 2 are bitopic proteins, whereas Type 3 proteins are polytopic.

Type 2 proteins are threaded into the lumen with the C terminus leading. The protein continues to be inserted until it reaches the hydrophobic stop signal sequence. Type 3 proteins are similar as Type 2, but they dispose multiple internal start and stop transfer sequences [17]. The “positive inside rule” declares that amino acid residues on the cytosolic side of the anchor sequence are positively charged and those on the luminal side of the hydrophobic transmembrane domain are negatively charged. The topology of a protein can be altered by mutating single positively charged amino acids on the cytoplasmic side and exchanging them with more negatively charged groups.

2.3. Outlook

11 β -HSD1 is located in the endoplasmatic reticulum membrane and is lumenally oriented. Mutants of 11 β -HSD1 having a single point mutation K5S in the hydrophobic anchor sequence, were shown to switch their topology to a cytoplasmic orientation of the catalytic domain [5](Figure 4). Surprisingly, this and other mutants with inverted topology retained wild-type activity in intact cells, using dehydrocorticosterone and cortisone as substrates. Therefore, the mutant enzyme with inverted topology did not reveal functional differences compared to wild-type 11 β -HSD1. The functional consequences of the luminal orientation can now be studied using the mutant construct.

Several substances are known inhibitors of 11 β -HSD1, such as carbenoxolone (CBX), glycyrrhetic acid (GA), chenodeoxycholic acid (CDCA) and flavanone [18]. GA and CBX inhibit 11 β -HSD1 in the nM range whereas CDCA and flavanone inhibit in the μ M range. Until now, most 11 β -HSD1 inhibitors are poorly characterized and experiments were mostly performed with lysates but not in intact cells. Testing these inhibitors in an 11 β -HSD1 profiling assay by comparing effects on wild-type and mutant 11 β -HSD1 enzyme may help to elucidate obscurities about these inhibitors. It is likely that some of these inhibitors will show potent inhibition of the cytoplasmic mutant K5S but only weak inhibition of luminal wild-type 11 β -HSD1 and vice versa. This may reveal that a particular inhibitor does not pass freely across the ER membrane and would function in a compartment specific way. In contrast, inhibitors may only act on the wild-type 11 β -HSD1 but not on the mutant K5S, indicating that the inhibitor is transported by vesicles from the plasma membrane directly to the ER-membrane, without having access to catalytic site of mutant K5S.

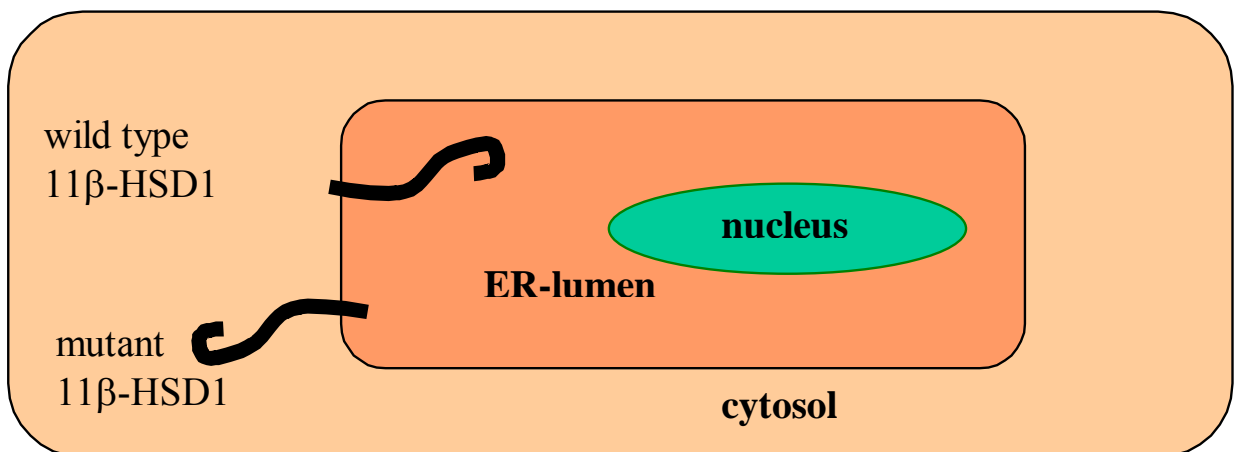


Figure 4

Schematic intracellular localization of wild type 11 β -HSD1 and 11 β -HSD1 mutant K5S. Wild type 11 β -HSD1 is luminal oriented whereas 11 β -HSD1 mutant K5S looks cytosolic. Inhibitors of wild type 11 β -HSD1 are forced to pass the plasmamembrane and the ER membrane. Inhibitors of 11 β -HSD1 mutant K5S should pass only the plasmamembrane.

2.4. References

1. White, P.C., T. Mune, and A.K. Agarwal, *11 beta-Hydroxysteroid dehydrogenase and the syndrome of apparent mineralocorticoid excess*. *Endocr Rev*, 1997. **18**(1): p. 135-56.
2. Stewart, P.M. and Z.S. Krozowski, *11 beta-Hydroxysteroid dehydrogenase*. *Vitam Horm*, 1999. **57**: p. 249-324.
3. New, M.I. and R.C. Wilson, *Steroid disorders in children: congenital adrenal hyperplasia and apparent mineralocorticoid excess*. *Proc Natl Acad Sci U S A*, 1999. **96**(22): p. 12790-7.
4. Kotelevtsev, Y., et al., *11beta-hydroxysteroid dehydrogenase type 1 knockout mice show attenuated glucocorticoid-inducible responses and resist hyperglycemia on obesity or stress*. *Proc Natl Acad Sci U S A*, 1997. **94**(26): p. 14924-9.
5. Odermatt, A., et al., *The N-terminal anchor sequences of 11beta-hydroxysteroid dehydrogenases determine their orientation in the endoplasmic reticulum membrane*. *J Biol Chem*, 1999. **274**(40): p. 28762-70.
6. Naray-Fejes-Toth, A. and G. Fejes-Toth, *Subcellular localization of the type 2 11beta-hydroxysteroid dehydrogenase. A green fluorescent protein study*. *J Biol Chem*, 1996. **271**(26): p. 15436-42.
7. Masuzaki, H., et al., *A transgenic model of visceral obesity and the metabolic syndrome*. *Science*, 2001. **294**(5549): p. 2166-70.
8. Agarwal, A.K., et al., *Cloning and expression of rat cDNA encoding corticosteroid 11 beta-dehydrogenase*. *J Biol Chem*, 1989. **264**(32): p. 18939-43.
9. Tannin, G.M., et al., *The human gene for 11 beta-hydroxysteroid dehydrogenase. Structure, tissue distribution, and chromosomal localization*. *J Biol Chem*, 1991. **266**(25): p. 16653-8.
10. Kurowski, M.A., et al., *Characterization of the cofactor-binding site in the SPOUT-fold methyltransferases by computational docking of S-adenosylmethionine to three crystal structures*. *BMC Bioinformatics*, 2003. **4**(1): p. 9.
11. Varughese, K.I., et al., *Structural and mechanistic characteristics of dihydropteridine reductase: a member of the Tyr-(Xaa)³-Lys-containing family of reductases and dehydrogenases*. *Proc Natl Acad Sci U S A*, 1994. **91**(12): p. 5582-6.
12. Mziaut, H., et al., *Targeting proteins to the lumen of endoplasmic reticulum using N-terminal domains of 11beta-hydroxysteroid dehydrogenase and the 50-kDa esterase*. *J Biol Chem*, 1999. **274**(20): p. 14122-9.
13. Agarwal, A.K., et al., *Expression of 11 beta-hydroxysteroid dehydrogenase using recombinant vaccinia virus*. *Mol Endocrinol*, 1990. **4**(12): p. 1827-32.
14. Blum, A., H.J. Martin, and E. Maser, *Human 11beta-hydroxysteroid dehydrogenase type 1 is enzymatically active in its nonglycosylated form*. *Biochem Biophys Res Commun*, 2000. **276**(2): p. 428-34.
15. Ozols, J., *Luminal orientation and post-translational modifications of the liver microsomal 11 beta-hydroxysteroid dehydrogenase*. *J Biol Chem*, 1995. **270**(5): p. 2305-12.
16. Walker, E.A., et al., *Functional expression, characterization, and purification of the catalytic domain of human 11-beta -hydroxysteroid dehydrogenase type 1*. *J Biol Chem*, 2001. **276**(24): p. 21343-50.
17. Wahlberg, J.M. and M. Spiess, *Multiple determinants direct the orientation of signal-anchor proteins: the topogenic role of the hydrophobic signal domain*. *J Cell Biol*, 1997. **137**(3): p. 555-62.
18. Schweizer, R.A., et al., *A rapid screening assay for inhibitors of 11beta-hydroxysteroid dehydrogenases (11beta-HSD): flavanone selectively inhibits 11beta-HSD1 reductase activity*. *Mol Cell Endocrinol*, 2003. **212**(1-2): p. 41-9.

**Specific Amino Acid Residues rather than Net Charge Distribution
Determine the Topology of 11 β -Hydroxysteroid Dehydrogenase Type 1
and the 50-kDa Esterase/Arylacetamide Deacetylase E3**

(Short title: Topology of 11 β -HSD1 and esterase E3)

Christoph Frick¹, Peter Arnold¹, Juris Ozols² and Alex Odermatt^{1*}

¹Division of Nephrology and Hypertension, Department of Clinical Research, University of Berne, 3010
Berne, Switzerland

²Biochemistry Department, University of Connecticut Health Center, Farmington, Connecticut 06030,
U.S.A.

*To whom correspondence should be addressed:

Dr. Alex Odermatt
Division of Nephrology and Hypertension
Department of Clinical Research
University of Berne
Freiburgstrasse 15
3010 Berne
Switzerland
Phone: +41 31 632 9438
Fax: +41 31 632 9444
E-mail: alex.odermatt@dkf2.unibe.ch

Summary

Previous studies have shown that the luminal orientation of the two type II endoplasmic reticulum (ER) membrane proteins 11 β -hydroxysteroid dehydrogenase type 1 (11 β -HSD1) and the 50 kDa-esterase/arylacetamide deacetylase (E3) is determined by their highly similar N-terminal transmembrane domains. Whereas substitution of Lys⁵ by Ser in 11 β -HSD1 led to an inverted topology of the enzyme in the ER-membrane, the topological determinants in E3 remained unknown. Here, we used immunohistochemistry and protease protection assays to analyze the topology of a series of mutant proteins. Our results demonstrate that in both enzymes a single lysine residue in their short cytoplasmic sequences, Lys⁵ in 11 β -HSD1 and Lys⁴ in E3, act as the major topological determinants. In addition, the negatively charged residues following on the C-terminal side of the transmembrane span, Glu²⁵ and Glu²⁶ in 11 β -HSD1 and Asp²⁵ in E3, play an important role for the determination of their luminal orientation. Our results suggest that the exact location of specific residues rather than the net charge distribution on either side of the transmembrane span determines their orientation in the ER-membrane. Furthermore, functional analysis of mutations in the N-terminal domain of 11 β -HSD1 revealed a 60% reduction of enzymatic activity when Glu²⁵ and Glu²⁶ were substituted by Lys and completely abolished catalytical activity when Lys³⁵ and Lys³⁶ were replaced by Ser, suggesting that these residues are responsible for the observed stabilizing effect of the N-terminal membrane anchor on the catalytic domain of 11 β -HSD1.

Introduction

In humans, 11 β -HSD1 catalyzes the reduction of biologically inactive cortisone to active cortisol, thereby playing an essential role in the local activation of the glucocorticoid receptor (GR). Recent animal experiments provided insight into the pathophysiological role of 11 β -HSD1. Mice deficient of 11 β -HSD1 were resistant to hyperglycemia induced by obesity or stress (1), whereas transgenic mice overexpressing 11 β -HSD1 developed visceral obesity with insulin resistance and dyslipidemia. In addition, overexpression of 11 β -HSD1 in adipose tissue caused salt-sensitive hypertension mediated by an activated renin-angiotensin system (2, 3). Therefore, 11 β -HSD1 is currently considered as a promising drug target for the treatment of diabetes type 2. Experiments in obese and diabetic mice treated with a specific 11 β -HSD1 inhibitor showed reduced blood glucose levels and increased insulin sensitivity (4, 5). In addition to its role in the activation of glucocorticoids, 11 β -HSD1 might play a role in the detoxification of reactive keto-compounds such as the potent tobacco carcinogen nicotine-derived nitrosamine ketone (NNK) and the anti-cancer drug oracin (6, 7). Despite its importance, relatively little is known about the molecular mechanisms by which 11 β -HSD1 exerts its physiological function.

11 β -HSD1 belongs to the family of short-chain dehydrogenases-reductases (SDR) (8, 9). SDRs are characterized by a core domain with conserved regions, including the Rossmann-fold for binding of the cofactor NADP(H) and the Tyr-(Xaa)₃-Lys motif in the catalytic site, which are flanked by less conserved N- and C-terminal sequences. We have previously shown that the single N-terminal transmembrane helix is responsible for the luminal orientation of the catalytic moiety of 11 β -HSD1 (10, 11). This stands in contrast to its counterpart 11 β -HSD2, which converts cortisol to cortisone and has three transmembrane spans determining cytoplasmic orientation in the ER-membrane. Several studies using 11 β -HSD1 constructs with N-terminal deletions demonstrated that this part of the enzyme is essential not only to anchor it to the ER-membrane but also for enzyme stability and activity (10, 12-14). However, the residues involved were not identified.

The N-terminal transmembrane span of 11 β -HSD1 is highly similar to that of the 50-kDa esterase/arylacetamide deacetylase (E3)(11), but otherwise the two proteins are unrelated (Figure 1). E3 is highly expressed in liver and adrenal glands and to a lesser extent in small intestine, stomach, kidney and pancreas (15). E3 acts as a N-deacetylase catalyzing hydrolytic reactions and plays a role in the prevention of arylamine-induced carcinogenesis (16). E3 might be involved, like the putative triacylglycerol hydrolase E1, in trafficking of apoB100 from ER to Golgi for secretion of hepatic very low density lipoprotein triacylglycerol (15). A significantly reduced expression of E3 is observed in insulin-deficient diabetes, which is characterized by a severe decrease in the secretion of hepatic very low density lipoprotein triacylglycerol. Both 11 β -HSD1 and E3 are exclusively expressed in the ER-

membrane and their N-terminal membrane anchors determine their luminal orientation (10, 11). Previous studies to identify the determinants for the topology of these enzymes revealed a role for Lys⁵ for the luminal orientation of 11 β -HSD1; however, substitution of the analogous Lys⁴ in E3 had no effect on topology, and the determinants for the luminal orientation of E3 remained unknown.

Here, we tested the hypothesis whether the negatively charged residues following the transmembrane span on the luminal side might be critical for the determination of the topology of these two enzymes. We evaluated also the role of charged amino acid residues in the N-terminal domain for enzymatic activity of 11 β -HSD1.

Materials and Methods

Materials

Cell culture reagents were purchased from Invitrogen, Basel, Switzerland. [1,2,6,7-³H]-corticosterone was from Amersham Pharmacia, Dübendorf, Switzerland. Fluorescence labelled antibodies were from Molecular Probes. Proteinase K was from Roche Diagnostics, Rotkreuz, Switzerland. All other chemicals were from Fluka AG, Buchs, Switzerland and were of the highest grade available.

Construction of Plasmids

The plasmid for expression of FLAG epitope-tagged human 11 β -HSD1 was constructed as described (10). Mutant 11 β -HSD1 constructs were generated by site-directed mutagenesis according to the Quick Change Mutagenesis kit (Stratagene, La Jolla, CA). The rabbit esterase E3-enhanced green-fluorescent protein (EGFP) chimera, containing the N-terminal membrane anchor sequence of E3 with a C-terminal EGFP, was constructed as described (11). For immunofluorescence experiments, a construct containing the N-terminal 34 amino acids of rabbit esterase E3 followed by a FLAG epitope-tag was generated by three-piece ligation of an *EcoRI-BamHI* fragment containing the N-terminal 34 amino acids of E3, a *BamHI-XbaI* fragment encoding the FLAG epitope (MDYKDDDD) and an *EcoRI-XbaI* pcDN3 expression vector fragment. Mutant E3-FLAG and -EGFP constructs were made by site-directed mutagenesis. All constructs were verified by sequencing.

Cell Culture and Transient Transfection

HEK-293 cells were grown in Dulbecco's modified Eagle's medium (DMEM) supplemented with 10% fetal calf serum, 4.5 g/l glucose, 50 units/ml penicillin, 50 mg/ml streptomycin and 2 mM glutamine. For microscopy experiments, cells were seeded at approximately 10% confluence onto glass coverslips

placed in six-well plates. After growth for 24 h at 37°C under 5% CO₂, cells were transfected with 2 µg/well of the corresponding expression plasmid and 1 µg/well EGFP-control plasmid. After incubation for 8 h, the medium was replaced to remove the Ca²⁺-phosphate precipitate. For isolation of microsomes and activity analysis, cells were seeded to 50% confluence in 10 cm dishes, transfected and medium replaced or cells washed three times with steroid-free DMEM (doubly charcoal treated).

Selective Permeabilization and Immunofluorescence Analysis

Immunofluorescence analysis was performed 48 h post-transfection as described previously (10). Briefly, paraformaldehyde (4%) fixed cells coexpressing the corresponding FLAG-tagged construct and EGFP control were washed four times with buffer NAPS (150 mM sodium phosphate, pH 7.4, 120 mM sucrose). For complete permeabilization of membranes, cells were blocked in NAPS buffer containing 1% milk powder and either 0.5% Triton X-100, for 11β-HSD1 constructs, or 1% saponin, for E3 constructs. For semipermeabilization of the plasma membrane, 25 µM digitonin was used. FLAG-tagged constructs were detected using anti-FLAG antibody M2 as primary antibody and ALEXA-594 goat anti-mouse secondary antibody. EGFP served as a transfection efficiency control. Following incubation with antibodies in NAPS containing 0.1% milk, samples were washed four times with NAPS and treated with Slow Fade Antifade kit (Molecular Probes). Samples were analyzed on a Carl Zeiss confocal microscope LSM410 (Carl Zeiss, Goettingen, Germany).

Isolation of Microsomes from HEK-293 Cells

HEK 293 cells were transfected with 8 µg of the corresponding expression plasmid per 10 cm dish. Cells from 4 dishes were collected 48 h post-transfection, washed with PBS, centrifuged at 150 × g for 3 min and the pellet resuspended in 1.2 ml buffer containing 10 mM Tris-HCl, pH 7.5, 0.5 M MgCl₂ and protease inhibitor (Complete, Roche). Cells were sonicated, 1.2 ml isotonic buffer (1 M sucrose, 10 mM Tris-HCl, pH 7.5, 2.5 M NaCl, 1 mM dithiothreitol (DTT)) added and lysates centrifuged at 1'000 × g for 10 min at 4 °C, followed by centrifugation at 11'000 × g for 10 min at 4 °C and 100'000 × g for 1 h at 4 °C. The pellet was resuspended in 300 µl buffer containing 10 mM Tris-HCl, pH 7.5, 0.5 M sucrose, 1.25 M NaCl and 0.5 mM DTT. The protein concentration was adjusted to 1 mg/ml, microsomal preparations shock frozen in liquid nitrogen and stored at -70 °C until analysis.

Protease Protection Assay and Immunoblotting

Microsomes (20 µg of total proteins) were incubated in a total volume of 25 µl with 0.25 µg/µl proteinase K (Roche) for 30 min on ice in the presence or absence of 0.5% Triton X-100. Proteinase K was inactivated by adding 2.5 µl of 10 mM phenylmethylsulfonyl fluoride in isopropanol for 5 min, followed by solubilization of proteins with SDS sample buffer and boiling for 5 min. Proteins were subjected to SDS-PAGE and Western blot analysis using anti-FLAG antibody M2 or anti-EGFP antibody as primary

antibodies and secondary horse-radish peroxidase conjugated antibody (Roche). Antibody binding was visualized using the ECL Western detection system (Pierce, Rockford, IL.).

Assay for 11 β -HSD

Oxidative activity of 11 β -HSD1 was measured as described previously (10). Briefly, the rate of conversion of corticosterone to 11-dehydrocorticosterone was determined in a final volume of 20 μ l containing 400 μ M NADP⁺, 30 nCi of [³H]-corticosterone and unlabeled corticosterone at different concentrations ranging from 12.5 nM to 800 nM. The reactions were started by mixing 10 μ l cell extract corresponding to 2-5 μ g of total proteins with 10 μ l reaction mixture and incubated for 10-20 min at 37°C. The reactions were stopped by adding an excess of unlabelled steroids in methanol, followed by separation of steroids by TLC. Enzyme kinetics were analyzed by the Eadie-Hofstee linear transformation of the Michaelis-Menten equation. Data represent mean \pm SD of at least four independent transfections.

Results

The cytoplasmic Lys⁴ and the luminal Asp²⁵ determine the topology of E3

In a previous study, we have shown restricted localization of E3 to the ER-membrane and luminal orientation of its catalytic moiety (11). The determinants for the topology of E3, however, remained unknown, and substitution by Ile for residue Lys⁴, which is analogous to Lys⁵ of 11 β -HSD1, did not affect its topology. Here, we subjected a construct, containing the N-terminal 34 amino acids of esterase E3 followed by a FLAG epitope for facilitated immunodetection, to site-specific mutagenesis and analyzed the orientation of the mutant proteins in the ER-membrane. Cells, coexpressing the corresponding FLAG-tagged construct and EGFP control protein, were subjected either to complete permeabilization of membranes by 0.5% Triton X-100 or to selective permeabilization of the plasma membrane using 25 μ M digitonin, followed by fluorescence microscopic detection. To investigate the role of negatively charged residues at the luminal side of the transmembrane helix, we replaced Asp²⁵, Glu²⁷ and Glu²⁸ in either wild-type or mutant K4I to Lys (Figure 2A).

The luminal orientation of E3 was not altered in the mutant containing Lys⁴, however, in mutant K4I substitution of negatively by positively charged Lys led to inverted insertion into the ER-membrane (Figure 3). Additional mutagenesis revealed that substitution of Asp/Glu/Glu to Asn/Gln/Gln or a single substitution of Asp²⁵ by Lys is sufficient to invert the topology of mutant K4I. All of the mutant proteins

analyzed showed exclusive localization to the ER-membrane. These results indicate that both Lys⁴ and Asp²⁵ are essential for the topology of E3 but not for ER retention. To confirm the effects on topology, microsomal vesicles expressing wild-type and mutant constructs consisting of the N-terminal 34 residues of E3 fused to EGFP were subjected to proteinase K digestion in the presence or absence of detergent (data not shown).

The luminal residues Glu²⁵ and Glu²⁶ are important determinants for the topology of 11 β -HSD1

Previous experiments identified Lys⁵ as an important determinant for the topology of 11 β -HSD1 (10). Substitution of Lys⁵ to Ser inverted the orientation of the catalytic moiety of 11 β -HSD1 from luminal to cytoplasmic. Here, we investigated the role of the luminal di-glutamate motif downstream of the transmembrane helix by analyzing a series of mutant 11 β -HSD1 constructs tagged at the C-terminus with a FLAG epitope (Figure 2B). Substitution of both Glu²⁵ and Glu²⁶ to Lys led to an inverted orientation of 11 β -HSD1 in the ER-membrane (Figure 4). When Glu²⁵ was replaced by Lys and Glu²⁶ by Gln, the orientation of the mutant 11 β -HSD1 was not altered, indicating that the change of charge at both positions is necessary to invert the topology of the enzyme. We have shown previously that mutant K5S but not K6S showed inverted topology. To test whether Lys⁶ also is involved in determination of topology, we mutated Glu²⁵ and Glu²⁶ in mutant K6S. Independent of the residue at position 6, the orientation of the enzyme was only inverted when both Glu²⁵ and Glu²⁶ were changed to Lys. These results indicate that Lys⁶ is not involved in determining the topology of 11 β -HSD1. In addition, all mutations analyzed in the present study did not alter the restricted expression of 11 β -HSD1 in the ER-membrane.

To confirm the effect of these mutations on the topology of 11 β -HSD1, microsomal vesicles were subjected to proteinase K digestion in the presence or absence of detergents. As seen in Figure 5, in intact vesicles mutants E25K/E26K and K6S/E25K/E26K were completely digested by proteinase K, whereas wild-type 11 β -HSD1 and all other mutants were protected from proteinase K-dependent digestion. Upon addition of Triton X-100, all constructs were digested. These results are consistent with the findings from fluorescence microscopic analyses of semipermeabilized cells, demonstrating an essential role of Glu²⁵ and Glu²⁶ for the membrane topology of 11 β -HSD1.

The effect of mutations in the N-terminal ER-membrane anchor of 11 β -HSD1 on enzymatic activity

Mutagenesis of the topological determinants at position 5/6 and 25/26 did not alter apparent K_m values of 11 β -HSD1, with values around 300 nM (Table 1), indicating that the orientation in the ER-membrane does not affect enzymatic activity. Except for mutant E25Q, all mutant enzymes with alterations in positions 25/26 showed a slight but significant reduction in their activity ($p < 0.05$). The least active mutants were K6S/E25K/E26K, K5S/K6S/E25K/E26K and E25K/E26K, followed by E25K/E25Q,

K6S/E25K/E26Q and E25Q/E26Q. Thus, there is a clear tendency for a loss of V_{\max} when substituting the negatively charged Glu residues first by polar Gln and then by positively charged Lys. All of the mutant enzymes showed exclusive localization to the ER-membrane, excluding a role of residues Glu²⁵ and Glu²⁶ as an ER retention signal.

Replacement of Lys³⁵ and Lys³⁶ by Ser neither affected ER-localization nor its orientation in the ER-membrane; however, it completely abolished enzymatic activity, demonstrating that Lys³⁵ and Lys³⁶ are essential for enzymatic activity of 11 β -HSD1.

Discussion

Cotranslational integration of proteins into the ER-membrane occur at sites termed translocons (17, 18). The ribosome synthesizing the polypeptide chain binds to the translocon, forming an aqueous pore through which the luminal domain of a membrane protein passes from the cytoplasm to the ER-lumen. The N-terminus of the growing polypeptide chain of type 2 transmembrane proteins stays on the cytoplasmic side, and the polypeptide chain is threaded into the ER-lumen with the C-terminus leading. The type II signal anchored ER-membrane proteins 11 β -HSD1 and E3 represent suitable models to study the determinants of membrane topology. Although they are otherwise unrelated, they share a highly similar N-terminal region consisting of a conserved Lys in the short cytoplasmic sequence, a membrane spanning helix with a cluster of Tyr residues and a segment of negatively charged amino acid residues C-terminal of the membrane span.

Charged residues in flanking regions often play a critical role in determining the topology of transmembrane helices, whereby positively charged residues show a strong preference for retention in the cytosol, while negatively charged residues have a weak affinity for translocation to the ER-lumen (19). According to the positive-inside rule, net charges on the polypeptide sequences flanking the transmembrane span determine the orientation, with the more positive of the two remaining on the cytoplasmic side of the membrane (20).

In the present study, we show that the topology of 11 β -HSD1 and E3 is determined by both a cytoplasmic conserved Lys and luminal, negatively charged amino acid residues. The topology of wild-type E3, with N-terminal charge +1 and C-terminal charge -3, when considering six residues downstream of the membrane span (+1/-3), and 11 β -HSD1 (+2/-2) is predicted by the positive-inside rule (Figure 6). However, the present analysis of several mutant proteins revealed that only some of the charged residues are critical and that their position plays an essential role.

We have previously shown that mutant K4I (0/-3) still adopts wild-type topology ($N_{\text{cyt}}/C_{\text{lum}}$)(11). Therefore, we now analyzed the role of luminal, negatively charged amino acid residues. Substitution of the three negatively charged residues that are closest to the membrane span by Lys in mutant D25K/E27K/E28K (+1/+3) did not alter its topology despite the excess of positive charges introduced at the C-terminal end of the membrane span. Thus, the topology of this mutant clearly does not follow the positive-inside rule. However, substitution of Asp²⁵ by Lys, K4I/D25K (0/-1), or of Asp²⁵ by Asn and Glu²⁵ and Glu²⁶ by Gln in mutant K4I, K4I/D25N/E27Q/E28Q (0/0), led to an inverted orientation in the ER-membrane. This indicates that Lys⁴ is the major determinant of E3 topology, whereby the introduction of several positively charged residues on the C-terminal end of the membrane span cannot overcome the dominant N-terminal signal. In mutants lacking the N-terminal signal, Asp²⁵, the negatively charged residue closest to the membrane span, dictates the topology.

That the topology of 11 β -HSD1 is determined by the appropriate charge at a specific position rather than by the net charge distribution is indicated by the fact that mutant K5S (+1/-2) adopts $N_{\text{lum}}/C_{\text{cyt}}$ topology, whereas K6S shows wild-type $N_{\text{cyt}}/C_{\text{lum}}$ orientation (10). The importance of Lys⁵ is also reflected by the fact that it is conserved in all known species, but Lys⁶ is replaced by Thr in squirrel monkey and by Asn in mouse. Substitution of Glu²⁵ and Glu²⁶ by Lys led to an inverted $N_{\text{lum}}/C_{\text{cyt}}$ orientation, indicating that in 11 β -HSD1 the introduction of two positive charges at the C-terminal side of the membrane span is dominant over the N-terminal Lys⁵ signal. This stands in contrast to E3, where the effect of Lys⁴ is not affected by the substitution of three negative by positive charges at the C-terminal side of the membrane span. In mutant K6S, like in wild-type 11 β -HSD1, both Glu²⁵ and Glu²⁶ had to be replaced by Lys to invert its topology, further demonstrating that Lys⁶ is not important for topology.

The localization of both 11 β -HSD1 and E3 is restricted to the ER-membrane, and their N-terminal transmembrane spans were sufficient to mediate retention in the ER-membrane (10, 11). Here, we show that removal by mutagenesis of the cytoplasmic Lys signal, the luminal negatively charged residues following C-terminal of the membrane helix or of Lys³⁵ and Lys³⁶ in 11 β -HSD1 does not affect retention in the ER-membrane, suggesting that intrinsic properties of the transmembrane sequence may be responsible. We have previously shown that mutations in the transmembrane Tyr motif did not affect restricted localization to the ER-membrane (10). A recent study by Blum et al. (13) demonstrated ER-membrane attachment of the truncated splice variant 11 β -HSD1B, lacking the transmembrane span, suggesting that the hydrophobic domain located at amino acid residues 136-158 also sufficiently mediates retention to the ER-membrane.

A fusion protein containing the transmembrane anchor of 11 β -HSD2 followed by residues 40-292 of 11 β -HSD1 as well as the truncated 11 β -HSD1 protein alone (residues 40-292, starting with Met-Thr-Gly) were catalytically inactive (10). This may be explained by the present finding that Lys³⁵ and Lys³⁶ are

absolutely required for enzymatic activity. The positive charge at positions 35/36 is highly conserved throughout different species with only cattle and sheep having Arg instead of Lys³⁶. Recently, Blum et al. (13) reported that the naturally occurring truncated splice-variant 11 β -HSD1B, lacking the first 30 amino acids but containing Lys³⁵ and Lys³⁶, could be partially reactivated upon solubilization from the microsomal fraction. Substitution of Val¹⁴⁹ by Arg in this truncated splice-variant rendered the protein more soluble; however, this protein was like 11 β -HSD1B not stable, indicating that the more N-terminal residues are required for the stability, e.g. for full activity of the enzyme. In line with this assumption, Walker et al. (12) purified a truncated enzyme lacking the first 23 amino acids, which retained activity. Since we found that mutagenesis of residues Glu²⁵ and Glu²⁶ led to a reduced V_{max}, which seems to be independent of the orientation of 11 β -HSD1 in the ER-membrane, these residues may play a role in stabilizing a conformationally active enzyme. Furthermore, Blum et al. (13) found that a construct missing the N-terminal 15 residues showed stable activity and both mutation of Val¹⁴⁹ to Arg or to Glu led to soluble, active forms of this truncated protein. This is supported by our previous finding that mutation of Tyr¹⁸⁻²¹ in the transmembrane helix led to a loss of activity (10), suggesting that the Tyr motif, which is conserved among species, with the exception of mouse containing only three Tyr residues, stabilizes the active conformation of 11 β -HSD1.

At present, the physiological consequences of the luminal orientation of 11 β -HSD1 still remain unclear. In *in vitro* assays, using intact HEK-293 cells transiently expressing 11 β -HSD1, the oxidation and reduction reaction are of comparable efficiency for both lumenally oriented wild-type enzyme and cytoplasmic mutant K5S. This is rather surprising since reductive conditions and cofactor NAD(H) are present in the cytoplasm whereas in the ER-lumen oxidative conditions and cofactor NADP(H) are predominant. However, 11 β -HSD1 accepts both cofactors with a slight preference for NADP(H), and neither glycosylation nor disulfide bridges are required for the catalytic activity of the enzyme (10, 21, 22). Thus, the HEK-293 expression system with comparable catalytic activities for mutant K5S and wild-type enzyme offers a suitable system to study the functional relevance of the luminal orientation of 11 β -HSD1. A successful 11 β -HSD1 inhibitor for the treatment of diabetes type 2 must enter the ER-lumen and inhibit the enzyme under luminal, oxidative conditions. The unspecific interference with the activities of cytoplasmic enzymes would be excluded if a pharmaceutical compound would be active only under oxidative but not reductive conditions.

In conclusion, our results suggest that (I) the orientation of 11 β -HSD1 and E3 in the ER-membrane is primarily determined by the conserved Lys in position 5 and 4, respectively, and, to a lesser extent, by the negatively charged Glu²⁵ and Glu²⁶ or Asp²⁵, respectively; (II) the ER-membrane retention of 11 β -HSD1 is a combination of intrinsic properties of the N-terminal anchor sequence and the membrane attachment

site between residues 136-158 and (III) the transmembrane Tyr motif, the di-glutamate motif and the di-lysine motif in the N-terminal anchor domain are essential for stabilization and activity of 11 β -HSD1.

References

1. Kotelevtsev, Y., Holmes, M. C., Burchell, A., Houston, P. M., Schmoll, D., Jamieson, P., Best, R., Brown, R., Edwards, C. R., Seckl, J. R., and Mullins, J. J. (1997) *Proc Natl Acad Sci U S A* *94*, 14924-9.
2. Masuzaki, H., Paterson, J., Shinyama, H., Morton, N. M., Mullins, J. J., Seckl, J. R., and Flier, J. S. (2001) *Science* *294*, 2166-70.
3. Masuzaki, H., Yamamoto, H., Kenyon, C. J., Elmquist, J. K., Morton, N. M., Paterson, J. M., Shinyama, H., Sharp, M. G., Fleming, S., Mullins, J. J., Seckl, J. R., and Flier, J. S. (2003) *J Clin Invest* *112*, 83-90.
4. Barf, T., Vallgarda, J., Emond, R., Haggstrom, C., Kurz, G., Nygren, A., Larwood, V., Mosialou, E., Axelsson, K., Olsson, R., Engblom, L., Edling, N., Ronquist-Nii, Y., Ohman, B., Alberts, P., and Abrahmsen, L. (2002) *J Med Chem* *45*, 3813-5.
5. Alberts, P., Nilsson, C., Selen, G., Engblom, L. O., Edling, N. H., Norling, S., Klingstrom, G., Larsson, C., Forsgren, M., Ashkzari, M., Nilsson, C. E., Fiedler, M., Bergqvist, E., Ohman, B., Bjorkstrand, E., and Abrahmsen, L. B. (2003) *Endocrinology* *144*, 4755-62.
6. Maser, E., Friebertshausen, J., and Volker, B. (2003) *Chem Biol Interact* *143-144*, 435-48.
7. Wsol, V., Szotakova, B., Skalova, L., and Maser, E. (2003) *Chem Biol Interact* *143-144*, 459-68.
8. White, P. C., Mune, T., and Agarwal, A. K. (1997) *Endocr Rev* *18*, 135-56.
9. Stewart, P. M., and Krozowski, Z. S. (1999) *Vitam Horm* *57*, 249-324.
10. Odermatt, A., Arnold, P., Stauffer, A., Frey, B. M., and Frey, F. J. (1999) *J Biol Chem* *274*, 28762-70.
11. Mziaut, H., Korza, G., Hand, A. R., Gerard, C., and Ozols, J. (1999) *J Biol Chem* *274*, 14122-9.
12. Walker, E. A., Clark, A. M., Hewison, M., Ride, J. P., and Stewart, P. M. (2001) *J Biol Chem* *276*, 21343-50.
13. Blum, A., Raum, A., and Maser, E. (2003) *Biochemistry* *42*, 4108-17.
14. Blum, A., and Maser, E. (2003) *Chem Biol Interact* *143-144*, 469-80.

15. Trickett, J. I., Patel, D. D., Knight, B. L., Saggerson, E. D., Gibbons, G. F., and Pease, R. J. (2001) *J Biol Chem* 276, 39522-32.
16. Probst, M. R., Beer, M., Beer, D., Jenö, P., Meyer, U. A., and Gasser, R. (1994) *J Biol Chem* 269, 21650-6.
17. Walter, P., and Johnson, A. E. (1994) *Annu Rev Cell Biol* 10, 87-119.
18. Ott, C. M., and Lingappa, V. R. (2002) *J Cell Sci* 115, 2003-9.
19. Harley, C. A., Holt, J. A., Turner, R., and Tipper, D. J. (1998) *J Biol Chem* 273, 24963-71.
20. von Heijne, G. (1992) *J Mol Biol* 225, 487-94.
21. Blum, A., Martin, H. J., and Maser, E. (2000) *Biochem Biophys Res Commun* 276, 428-34.
22. Arnold, P., Tam, S., Yan, L., Baker, M. E., Frey, F. J., and Odermatt, A. (2003) *Mol Cell Endocrinol* 201, 177-87.

Footnotes

The abbreviations used are: 11 β -HSD, 11 β -hydroxysteroid dehydrogenase; DMEM, Dulbecco's modified Eagle's medium; DTT, dithiothreitol; E3, 50-kDa esterase/arylacetamide deacetylase; EGFP, enhanced green-fluorescent protein; ER, endoplasmic reticulum; GR, glucocorticoid receptor; HEK, human embryonic kidney; SDR, short-chain dehydrogenases-reductases; TLC, thin-layer chromatography.

Acknowledgements

This work was supported by grants from the Cloëtta Research Foundation and the Swiss National Science Foundation (No 3100AO-100060). We thank Mario Ziegler for excellent technical support.

Table I

Oxidation of cortisosterone by wild-type and mutant 11 β -HSD1 enzymes

Oxidation of cortisosterone by lysates of HEK-293 cells transfected with 11 β -HSD constructs was determined as described under “Materials and Methods”. Activities are expressed in terms of apparent K_m and apparent V_{max} . Data were obtained from 4-8 independent experiments and are presented as mean \pm S.D.

Construct	K_m^a	$V_{max}^{a,b}$
11 β -HSD1 (wild-type)	308 \pm 92	4.9 \pm 1.5
E25Q	342 \pm 96	5.2 \pm 0.9
E25K	294 \pm 89	3.1 \pm 1.4
E26K	338 \pm 75	3.5 \pm 0.4
K6S/E25K	302 \pm 105	3.0 \pm 0.4
E25Q/E26Q	289 \pm 72	2.4 \pm 0.7
K6S/E25Q/E26Q	278 \pm 69	2.7 \pm 0.4
E25K/E25Q	319 \pm 50	2.2 \pm 0.6
K6S/E25K/E26Q	321 \pm 71	2.2 \pm 0.4
E25K/E26K	328 \pm 92	2.0 \pm 0.9
K6S/E25K/E26K	317 \pm 53	0.9 \pm 0.5
K5S/K6S/E25K/E26K	302 \pm 96	1.7 \pm 0.3
K35S/K36S	n.d. ^c	n.d. ^c

^a Apparent K_m (nM) and apparent V_{max} (nM/h \times mg of total protein) were calculated according to Eadie-Hofstee, assuming the reaction follows first-order rate kinetics (Hill coefficients ranging between 0.93 and 1.15).

^b For calculation of V_{max} the amount of 11 β -HSD protein per mg of total proteins was determined semiquantitatively by densitometric analysis of Western blots, whereby each FLAG-tagged mutant was compared with the value obtained for FLAG-tagged wild-type 11 β -HSD1.

^c Activity not detectable despite normal expression level.

Figure Legends

Figure 1. Schematic representation of the N-terminal membrane anchoring region of 11 β -HSD1 and E3.

Figure 2. Wild-type and mutant constructs of rabbit 50-kDa esterase/arylacetamide deacetylase E3 and human 11 β -HSD1. The name of the mutant protein is given on the left, mutated residues are in italic and bold, and the orientation of the corresponding construct in the ER-membrane is indicated on the right.

Figure 3. Orientation in the ER-membrane of constructs containing wild-type or mutant membrane anchoring regions of rabbit 50-kDa esterase/arylacetamide deacetylase E3. Wild-type or mutant proteins indicated on the top of each lane were coexpressed with enhanced green-fluorescent protein (EGFP) in HEK-293 cells. Plasma membranes of cells were selectively permeabilized with digitonin (first two rows) or membranes completely permeabilized with 1% saponin (row 3 and 4), followed by detection of the C-terminally attached FLAG epitope by mouse monoclonal anti-FLAG antibody M2 and secondary fluorescent ALEXA-594 anti-mouse antibody using confocal microscopy.

Figure 4. Orientation of wild-type or mutant 11 β -HSD1 in the ER-membrane. HEK-293 cells were cotransfected with C-terminally FLAG-tagged wild-type or mutant 11 β -HSD1 (indicated at the top of each lane) and EGFP. Cells were either completely permeabilized with 0.5% triton X-100 (row 3 and 4), or the plasma membrane was selectively permeabilized using 25 μ M digitonin (row 1 and 2), allowing restricted access of the antibody to the cytosolic compartment.

Figure 5. Proteinase K sensitivity of wild-type and mutant 11 β -HSD1 in ER-microsomes. HEK-293 cells were transfected with FLAG epitope-tagged wild-type 11 β -HSD1 (A), mutant E25K/E26K (B), K6S/E25K/E26Q (C), E25K/E26Q (D) or K6/E25K/E26K (E), and microsomal vesicles were isolated as described under Materials and Methods. Microsomal preparations were incubated for 30 min at 4°C in the presence (+) or absence (-) of 0.25 μ g/ μ l proteinase K and 0.5% Triton X-100. Proteins were separated on 12.5% SDS-PAGE, transferred to nitrocellulose, followed by detection with mouse monoclonal anti-FLAG antibody M2 and secondary anti-mouse HRP antibody.

Figure 6. Models showing the orientation of 11 β -HSD1 and E3 constructs in the ER-membrane. A, in wild-type 11 β -HSD1 Lys⁵ acts as a signal to retain the N-terminus in the cytoplasm. The C-terminal catalytic moiety then is guided through the translocon to the ER-lumen. In mutant E25K/E26K, the two lysine residues prevent the C-terminal catalytic domain from passing through the ER-membrane. The N-

terminal segment containing Lys⁵ then flips to the luminal side and stabilizes the protein in a N_{lum}/C_{cyt} orientation in the ER-membrane. *B*, In E3 Lys⁴ retains the N-terminus on the cytoplasmic side and the growing polypeptide is guided through the translocon into the ER-lumen. In mutant K4I/D25K Lys⁴ is absent and the N-terminal segment passes through the translocon to the ER-lumen and stabilizes the protein in a N_{lum}/C_{cyt} orientation in the ER-membrane.

A) esterase E3

RE3	M G V K T V L L L I V G V L G A Y Y V Y T P L P D N I E E P W R L L	luminal
K4I	M G V I T V L L L I V G V L G A Y Y V Y T P L P D N I E E P W R L L	luminal
K4I/D25N/E28Q/E29Q	M G V I T V L L L I V G V L G A Y Y V Y T P L P N N I Q Q P W R L L	cytoplasmic
K4I/D25K/E28K/E29K	M G V I T V L L L I V G V L G A Y Y V Y T P L P K N I K K P W R L L	cytoplasmic
K4I/D25K	M G V I T V L L L I V G V L G A Y Y V Y T P L P K N I E E P W R L L	cytoplasmic
D25K/E28K/E29K	M G V K T V L L L I V G V L G A Y Y V Y T P L P K N I K K P W R L L	luminal
D25N/E28Q/E29Q	M G V K T V L L L I V G V L G A Y Y V Y T P L P N N I Q Q P W R L L	luminal

B) 11β-HSD1

11βHSD1	M A F M K K Y L L P I L G L F M A Y Y Y Y S A N E E F R P E M L Q G K K V	luminal
E25Q	M A F M K K Y L L P I L G L F M A Y Y Y Y S A N Q E F R P E M L Q G K K V	luminal
E25Q/E26Q	M A F M K K Y L L P I L G L F M A Y Y Y Y S A N Q Q F R P E M L Q G K K V	luminal
E25K/E26K	M A F M K K Y L L P I L G L F M A Y Y Y Y S A N K K F R P E M L Q G K K V	cytoplasmic
E25K	M A F M K K Y L L P I L G L F M A Y Y Y Y S A N K E F R P E M L Q G K K V	luminal
K6S/E25K/E26K	M A F M K S Y L L P I L G L F M A Y Y Y Y S A N K K F R P E M L Q G K K V	cytoplasmic
K5S/K6S/E25K/E26K	M A F M S S Y L L P I L G L F M A Y Y Y Y S A N K K F R P E M L Q G K K V	cytoplasmic
K6S/E25K	M A F M K S Y L L P I L G L F M A Y Y Y Y S A N K E F R P E M L Q G K K V	luminal
K6S/E25Q/E26Q	M A F M K S Y L L P I L G L F M A Y Y Y Y S A N Q Q F R P E M L Q G K K V	luminal
E25K/E26Q	M A F M K K Y L L P I L G L F M A Y Y Y Y S A N K Q F R P E M L Q G K K V	luminal
E26K	M A F M K K Y L L P I L G L F M A Y Y Y Y S A N E K F R P E M L Q G K K V	luminal
K6S/E25K/E26Q	M A F M K S Y L L P I L G L F M A Y Y Y Y S A N K Q F R P E M L Q G K K V	luminal
K35S/K36S	M A F M K K Y L L P I L G L F M A Y Y Y Y S A N E E F R P E M L Q G S S V	luminal

Figure 2

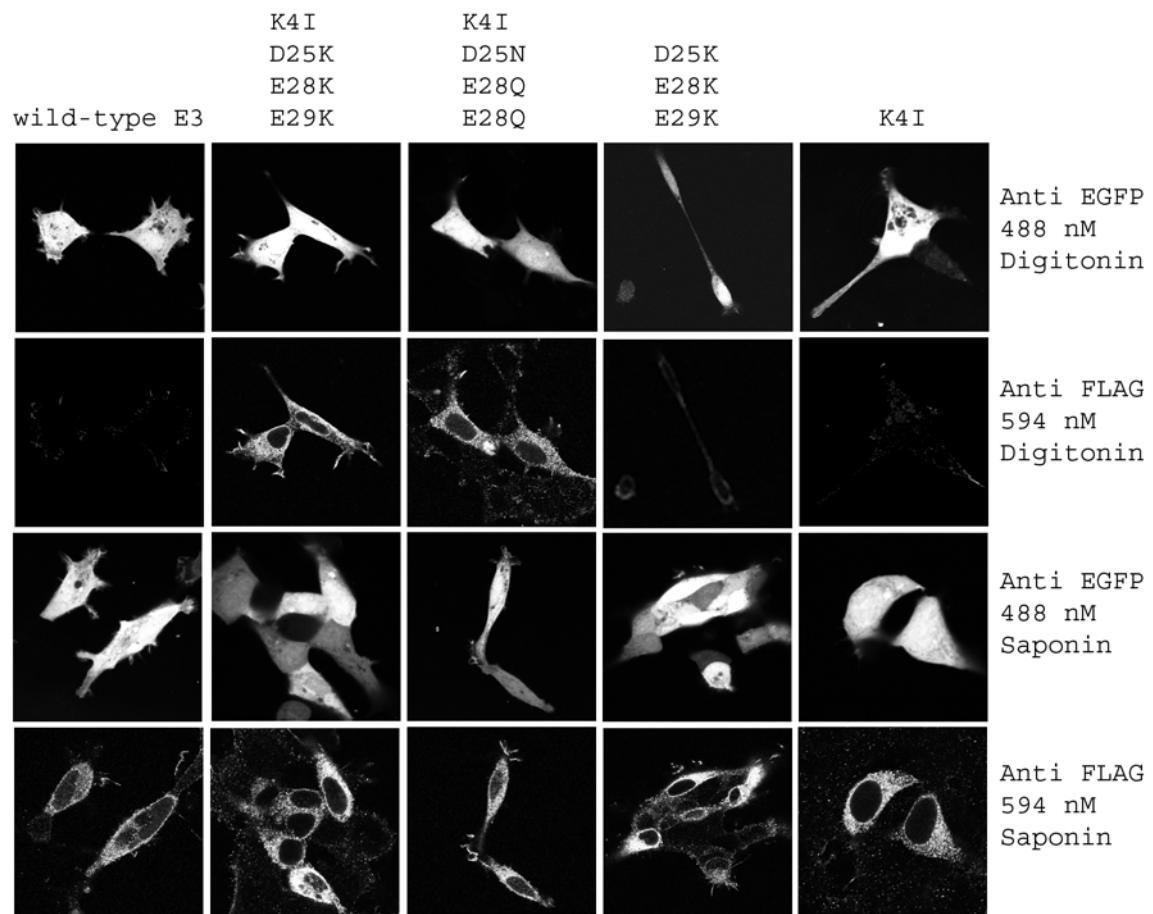


Figure 3

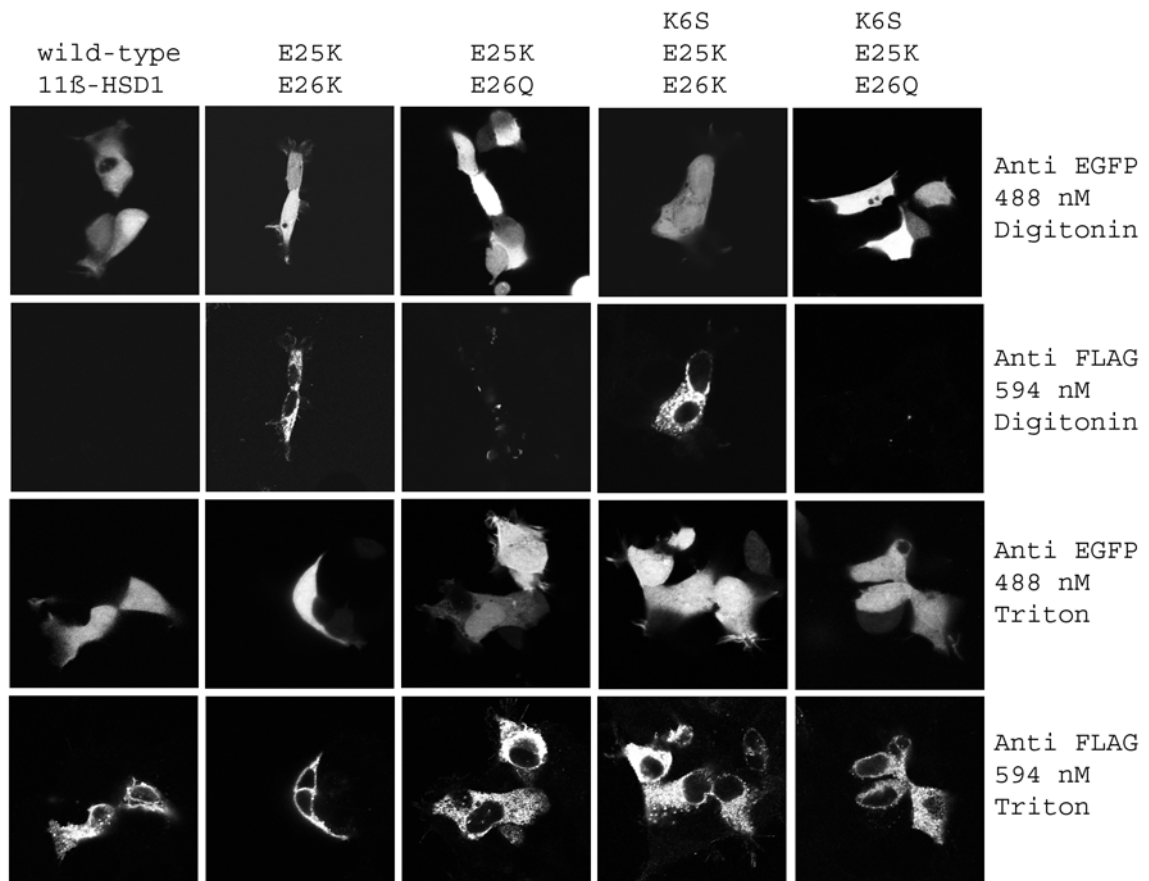


Figure 4

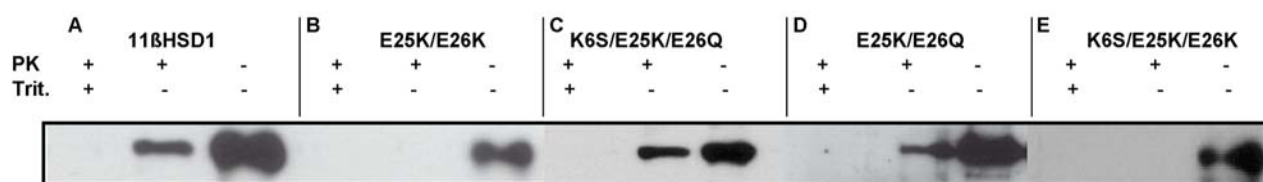


Figure 5

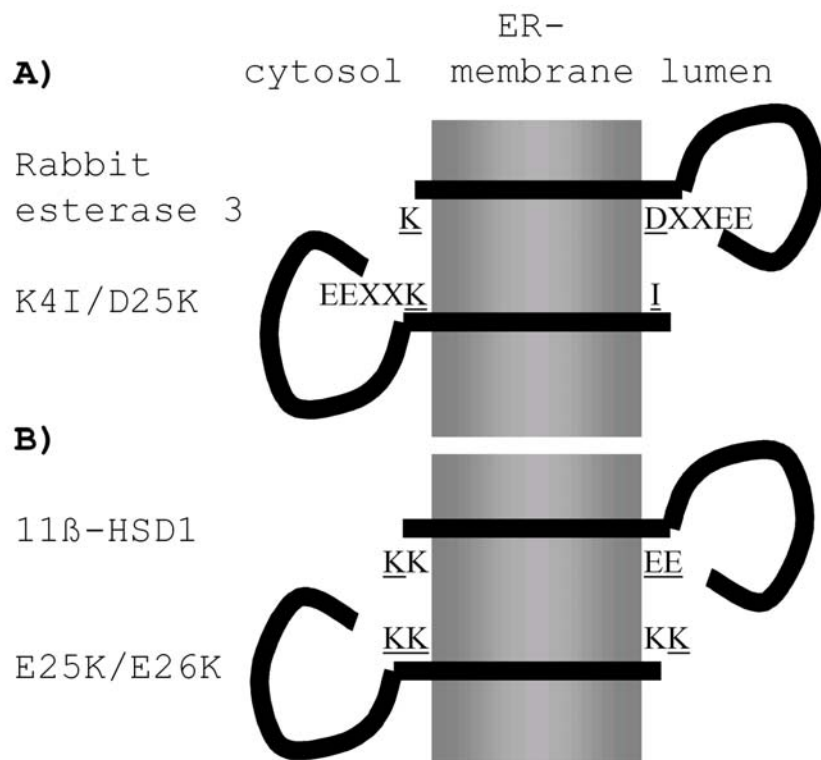


Figure 6

4. Acknowledgement

I would like to thank Alex Odermatt for guiding me through my PhD thesis. Under his supervision, I could work quite independently but without missing his competent support whenever I needed it. During this past few years I learned a lot from him in the field of research, and I specially appreciate the friendly atmosphere between us.

A big "thank you" goes to Charles Parkos from the Emory University in Atlanta for supporting me in a fascinating collaboration and for having his scientific and moral support.

I also would like to thank Luca Mazzucchelli for scientific assistance and for writing the coreferat for my thesis.

I thank Prof. Thomas Seebeck for acting as an expert and for his support in the present work.

I would like to thank Profs. Brigitte and Felix Frey for their support and giving me the opportunity to do my PhD thesis in their laboratory.

A special thank goes to former PhD students as well as to all present PhD students, Postdocs and technicians from the Odermatt-Group and Frey-Lab.

I gratefully thank my parents Luise and Karl Frick and my sister Franziska Frick for loving and supporting me ever since I exist.

Sincere thanks I give to my friends in Liechtenstein and Berne accompanying me through the ups and downs during my PhD and for powerful friendship.

5. Curriculum Vitae

PERSONAL DATA

Christoph Anton Frick
May 25, 1976, St.Gallen (Switzerland)
Gesellschaftsstrasse 81
3012 Bern,
Switzerland

christoph.frick.1@student.unibe.ch

EDUCATION/PROMOTION

- | | |
|-----------|--|
| 2001-2004 | PhD thesis, Division of Nephrology and Hypertension
University of Berne, Inselspital |
| 1999-2000 | Diploma thesis, Division of Nephrology and Hypertension
University of Berne, Inselspital |
| 1996-2000 | Studies in Biology, specialization in microbiology,
Department of Microbiology, University of Berne |
| 1988-1996 | Gymnasium (economics), Vaduz, Principality of Liechtenstein |

PROFESSIONAL ACTIVITY

- | | |
|------|---|
| 1996 | Poster presentation at the day of Clinical Research, Berne |
| 2001 | Poster presentation at the international Society of Nephrology (ISN)
San Francisco, CA |
| 1998 | 3-month training in Prof. T. Wang laboratory at Stanford, CA |
| 1997 | 3-month training in Prof. C. Parks laboratory at the
University of North Carolina, Chapel Hill, NC |
| 1996 | 3-month training in Prof. C. Parks laboratory at the
University of North Carolina, Chapel Hill, NC |

PUBLICATIONS

PUBLISHED PAPERS

Selection of peptide ligands binding to the basolateral cell surface of proximal convoluted tubules,

Kidney Int (2002)

Audige, A. Frick, C., Frey, F. J., Mazzucchelli, L., Odermatt, A.

Identification of receptor ligands by screening phage-display peptide libraries ex vivo on microdissected kidney tubules,

J Am Soc Nephrol (2001)

Odermatt, A., Audige, A., Frick, C., Vogt, B., Frey, B. M., Frey, F. J., Mazzucchelli, L.

PAPERS IN PREPARATION

Specific Amino Acid Residues rather than Net Charge Distribution

Determine the Topology of 11 β -Hydroxysteroid Dehydrogenase

Type 1 and the 50-kDa Esterase/Arylacetamide Deacetylase E3

Frick, C., Arnold, P., Ozols, J., Odermatt, A.

Selection of a high affinity peptide ligand binding to a novel functional site of β 2 Integrin p150

Frick, C., Odermatt, A., Edens, H., Zen, K., Geigerman, C.,

Portmann, R., Fuller, R.E., Mazzucchelli, L., Jaye, D.L., and Parkos, C.A.